

Scalable Safe Exploration for Global Optimization of Dynamical Systems

Bhavya Sukhija^a, Matteo Turchetta^a, David Lindner^a, Andreas Krause^a,
Sebastian Trimpe^b, Dominik Baumann^{b,c}

^a*Department of Computer Science, ETH Zürich, Switzerland*

^b*Institute for Data Science in Mechanical Engineering, RWTH Aachen University, Germany*

^c*Department of Information Technology, Uppsala University, Sweden*

Abstract

Learning optimal control policies directly on physical systems is challenging since even a single failure can lead to costly hardware damage. Most existing learning methods that guarantee safety, i.e., no failures, during exploration are limited to local optima. A notable exception is the GOSAFE algorithm, which, unfortunately, cannot handle high-dimensional systems and hence cannot be applied to most real-world dynamical systems. This work proposes GOSAFEOPT as the first algorithm that can safely discover globally optimal policies for complex systems while giving safety and optimality guarantees. Our experiments on a robot arm that would be prohibitive for GOSAFE demonstrate that GOSAFEOPT safely finds remarkably better policies than competing safe learning methods for high-dimensional domains.

Keywords: Model-free learning, Bayesian Optimization, Safe learning.

1. Introduction

The traditional approach to controlling a dynamical system consists in deriving a mathematical model and designing a policy based on it. The increasing complexity of modern technical systems makes this approach forbiddingly involved and time-consuming. Model-free reinforcement learning (RL) methods [1] are a promising alternative to this approach as they circumvent the modeling step by learning control policies directly from data. To suc-

Email addresses: bhavya.sukhija@inf.ethz.ch (**Bhavya Sukhija**),
matteo.turchetta@inf.ethz.ch (**Matteo Turchetta**), david.lindner@inf.ethz.ch (**David Lindner**),
krausea@ethz.ch (**Andreas Krause**), trimpe@dsme.rwth-aachen.de (**Sebastian Trimpe**),
dominik.baumann@it.uu.se (**Dominik Baumann**)

ceed, they need to explore the system and its environment. Without a model, this can be arbitrarily risky and violate safety constraints, ultimately damaging the system. Since modern hardware such as robotics is expensive and its repair is time-consuming, safe exploration is crucial to apply model-free RL to real-world problems.

In this paper, we propose GOSAFEOPT, an algorithm that can search for globally optimal policies in complex systems without the need for a dynamics model while guaranteeing safe exploration.

1.1. Related Work

Model-free RL has achieved remarkable results on a variety of tasks such as mastering Atari games [2] or learning complex locomotion behaviors [3]. However, most of these works consider virtual environments, e.g., games or simulations of dynamical systems. To take full advantage of model-free RL, it is necessary to deploy these methods in the real world, where safety becomes a concern. This has sparked a significant amount of research on safe learning [4; 5; 6; 7; 8]. For instance, [9] extends the trust region policy optimization algorithm [10] to constrained Markov decision processes (CMDPs) [11], where safety is formulated as constraints on costs incurred by a policy. The authors of [12] incorporate safety guarantees during training for a series of dynamic programming [13] and RL algorithms, such as Deep Q-learning [14], through Lyapunov functions. The work in [15] learns a safety critic to predict the probability of failure given a state and action pair and imposes constraints on this probability. However, these methods suffer from the notoriously poor sample complexity of deep model-free RL, which makes them impractical for learning directly on real hardware systems.

Alternatively, Bayesian optimization (BO) [16] provides a suite of black-box optimization algorithms, which, due to their sample efficiency, have been successfully applied to search for optimal policies on real hardware systems [17; 18; 19; 20]. BO naturally captures safety-critical scenarios by augmenting the optimization problem with constraints [21; 22; 23; 24; 25; 26; 27; 28; 29], which are usually unknown *a priori* and learned from data collected during experiments. In constrained BO, there are two main classes of methods. On the one hand, approaches like [21; 22; 18] find safe solutions while allowing unsafe evaluations during training. While this is acceptable for some applications, this is not the case when

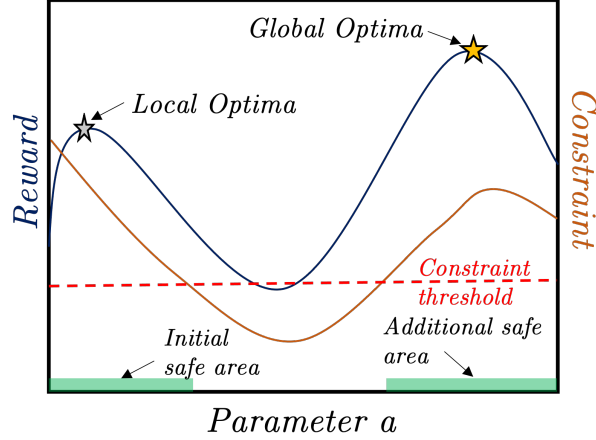


Figure 1: Illustrative example with disjoint safe regions. *The blue line depicts the objective, the orange line the constraint function, and the red dotted line the constraint threshold. There are two safe regions that are marked in green. SAFEOPT cannot explore the global optimum if it is initialized in the left region.*

dealing with expensive hardware. On the other hand, methods like [25; 26] guarantee safe exploration by exploiting properties of the constraint functions, e.g., regularity. In particular, SAFEOPT [25] has been extensively used for safe policy search [23; 24; 28]. Starting from an initial safe policy, it runs experiments to gradually expand the set of policies considered safe (safe set). Since this expansion is inherently local, SAFEOPT is limited to exploring a safe set connected with the initial safe policy. Therefore, it could miss the global optimum in presence of disjoint safe regions (see Fig. 1). Disjoint safe regions appear when learning an impedance controller for a robot arm, as we show in our experiments, and in many other applications [30; 17; 29]. To address this limitation, [29] proposes GOSAFE, which can provably and safely discover the safe global optimum in presence of disjoint safe regions under mild conditions. To achieve this, it learns safe backup policies for different states and uses them to preserve safety when evaluating policies outside of the safe set. To this end, it actively explores the joint space of states and policies, which is infeasible for all but the simplest systems with low-dimensional state spaces ([31] argues that an overall dimension, i.e., parameter and state space, $d > 3$ is already challenging). As a result, GOSAFE cannot be applied to general complex dynamical systems.



Figure 2: Franka Emika panda; seven degree of freedom robot arm used for our evaluations.

1.2. Contributions

This work presents GOSAFEOPT, the first algorithm that can globally search for optimal policies for safety-critical, complex dynamical systems, i.e., systems with high-dimensional state spaces. Crucially, GOSAFEOPT leverages the *Markov property* of the system’s state to learn backup policies without actively exploring in the state space and uses these backup policies to guarantee safety when evaluating policies outside of the safe set. We provide high-probability safety guarantees for GOSAFEOPT and we prove that it recovers the safe globally optimal policy for many practical cases. Finally, we validate it in simulated and real safety-critical path following experiments on a robotic arm (see Fig. 2), which is too complex for competing global safe search methods. Further, we show that GOSAFEOPT achieves remarkably better performance compared to existing methods for safe policy search for high-dimensional problems.

Table 1 compares GOSAFEOPT to prior work on safe exploration discussed in Section 1.1 in terms of safety guarantees, scalability, global exploration, and sample efficiency. It shows that GOSAFEOPT is the only method that can do sample-efficient global exploration in high-dimensional systems while providing safety guarantees.

The rest of the paper is organized as follows: after defining the problem setting and introducing preliminaries in Sections 2 and 3 respectively, we analyze the drawbacks of prior work in Section 3.5. In Section 4, we present GOSAFEOPT as a solution to these drawbacks,

Table 1: Comparison between GoSAFEOPT and prior work on safe exploration based on their safety guarantees, scalability, global exploration, and sample efficiency.

	Safe exploration	High-dimensional state space	Global exploration	Sample efficient
SAFEOPT [24]	✓	✗	✗	✓
SAFEOPTSWARM [32]	✓	✓	✗	✓
SAFELINEBO [31]	✓	✓	✗	✓
GoSAFE [29]	✓	✗	✓	✗
GoSAFEOPT (ours)	✓	✓	✓	✓

and provide safety and, optimality guarantees for it. Finally, we demonstrate on software and hardware the superiority of GoSAFEOPT over existing methods for safe policy search for high-dimensional problem in Section 5.

2. Problem Setting

We consider an unknown, Lipschitz-continuous system

$$dx(t) = z(x(t), u(t)) dt, \tag{1}$$

where, $z(\cdot)$ represents the system dynamics, $x(t) \in \mathcal{X} \subset \mathbb{R}^s$ is the system state and $u(t) \in \mathcal{U} \subset \mathbb{R}^p$ is the input we apply to steer the system state to follow a desired trajectory $x_{\text{des}}(t) \in \mathcal{X}$ starting from an initial condition $x(0) = x_0$.

The control input $u(t)$ to apply in a given state $x(t)$ is specified by a policy $\pi : \mathcal{X} \times \mathcal{A} \rightarrow \mathcal{U}$, with $u(t) = \pi(x(t), a) = \pi^a(x(t))$. The policy is parameterized by parameters a , which belong to a finite parameter space $\mathcal{A} \subset \mathbb{R}^d$. Our goal of making the system follow the desired trajectory $x_{\text{des}}(t)$ is quantified through an objective function, $f : \mathcal{A} \rightarrow \mathbb{R}$, which we optimize with respect to the policy parameters, a . Since the dynamics of the system in Eq. (1) are unknown, so is the objective f . Nonetheless, we can deploy a policy with parameter a , obtain a noisy measurement of $f(a)$, and use this information to find better policies. Unfortunately, when deploying a new policy on an unknown system, we cannot predict the consequences. In safety-critical systems, this may lead to harmful outcomes that damage the system and its surroundings. In these cases, we can formulate safety as a set of *unknown* constraints over the system trajectories that must be satisfied *at all times*. Since the trajectory of a deterministic system (1) is fully determined by its initial state and the control policy, these

constraints take the form $g_i : \mathcal{A} \times \mathcal{X} \rightarrow \mathbb{R}$, i.e., $g_i(a, x)$. When considering the nominal initial condition x_0 , we omit the dependency on the state x_0 and write $g_i(a)$ for simplicity. The resulting constrained optimization problem with unknown objective and constraints is:

$$\max_{a \in \mathcal{A}} f(a) \quad \text{subject to} \quad g_i(a) \geq 0, \forall i \in \{1, \dots, q\}. \quad (2)$$

Clearly, solving this problem without incurring failures for generic systems, objectives, and constraints is a hopeless task. The following section introduces the assumptions we make when developing our method.

2.1. Assumptions

To solve the problem in Eq. (2), we must learn about the objective and the constraints without incurring failures. To start collecting data safely, we must be provided with at least one initial safe policy, which, in reality, could be derived from simulators or simple first principles models.

Assumption 1. A set S_0 of safe parameters for initial condition x_0 is known.

In practice, similar policies often lead to similar outcomes. In other words, the objective and the constraints exhibit some smoothness properties, which we capture through their reproducing kernel Hilbert space (RKHS) [33] norm.

Assumption 2. The objective f and the constraints g_i have bounded norm in a RKHS associated to a kernel k , $\|f\|_k \leq B$ and $\|g_i\|_k \leq B$, and are Lipschitz continuous with known constants.

Crucially, this assumption lets us infer the safety of unobserved policies.

While f and g_i are unknown, we assume we receive noisy measurements of both. We now formalize our assumptions on the measurement model.

Assumption 3. The measurement noise is σ -sub-Gaussian, i.e., $y_f = f(a) + \epsilon$ with ϵ σ -sub-Gaussian. Similarly, we have $y_{g_i} = g_i(a) + \epsilon_{g_i}$ with ϵ_{g_i} σ -sub-Gaussian for all $i \in \{1, \dots, q\}$.

Assumptions 1, 2, and 3 are common in the safe BO literature [23; 24; 25]. However, these approaches treat the evaluation of a policy as a black box. In contrast, we monitor the rollout

of a policy to intervene and bring the system back to safety if necessary. For our interventions to be effective, the future trajectory of the system must depend only on its current state and not the past ones, i.e., the system must be Markovian [34]. This is a typical assumption in RL [1] and is fulfilled for our system in Eq. (1), as we show in Proposition 1 in the appendix.

Unfortunately, a Markovian system is not sufficient to guarantee the safety of the whole trajectory. Consider the case where safety is expressed as a constraint on a cost accumulated along the trajectory like for standard CMDPs. Even if the two sub-trajectories (pre and post-intervention) are individually safe, their union may not be. Therefore, we must limit the types of constraints we consider.

Assumption 4. Consider an instantaneous state-dependent constraint function $\bar{g}_i(x(t))$. We assume that the constraint function $g_i(a, x_0)$ is also state-dependent and for all $i \in \{1, \dots, q\}$ defined as

$$g_i(a, x_0) = \min_{x' \in \xi_{(0, x_0, a)}} \bar{g}_i(x'), \quad (3)$$

with $\xi_{(0, x_0, a)} := x_0 + \int_0^t z(x(\tau); \pi^a(x(\tau))) dt$ the trajectory of $x(t)$ under policy parameter a starting from x_0 at time 0.

An example of such a constraint is the minimum distance to an obstacle.

Given Assumption 4, we can now provide a formal safety definition.

Definition 1. An experiment is safe if, for all $t \geq 0$ and all $i \in \{1, \dots, q\}$,

$$\bar{g}_i(x(t)) \geq 0. \quad (4)$$

3. Preliminaries

This section reviews GPs and how to use them to construct calibrated confidence intervals, as well as relevant prior work on safe exploration, i.e., SAFEOPT and GOSAFE.

3.1. Gaussian Processes

To predict the reward and safety of a policy before deploying it, we want to build a model of $f(a)$ and $g_i(a)$. To this end, we model our reward and constraints using Gaussian

process regression (GPR) [35], which uses Bayes rule to combine our prior belief and the data we collect. In GPR, our prior belief is captured by a GP, which is fully determined by a prior mean function¹ and a kernel $k(a, a')$. Importantly, if the observations are corrupted by independent and identically distributed (i.i.d) Gaussian noise with variance σ^2 , i.e., $y_i = f(a_i) + v_i$, and $v_i \sim \mathcal{N}(0, \sigma^2)$, the posterior over f is also a GP whose mean and variance can be computed in closed form. Let us denote with $Y_n \in \mathbb{R}^n$ the array containing n noisy observations of f , then the posterior of f at a^* , is $f(a^*) \sim \mathcal{N}(\mu_n(a^*), \sigma_n^2(a^*))$:

$$\mu_n(a^*) = k_n(a^*) (K_n + I_n \sigma^2)^{-1} Y_n, \quad (5a)$$

$$\sigma_n^2(a^*) = k(a^*, a^*) - k_n(a^*) (K_n + I_n \sigma^2)^{-1} k_n^T(a^*), \quad (5b)$$

where, the entry $i, j \in \{1, \dots, n\} \times \{1, \dots, n\}$ of the covariance matrix $K_n \in \mathbb{R}^{n \times n}$ is $k(a_i, a_j)$, $k_n(a^*) = [k(a^*, a_1), \dots, k(a^*, a_n)]$ captures the covariance between x^* and the data, and I_n is the $n \times n$ identity matrix.

Eq. (5) considers the case where f is a scalar function. However, we aim to model the objective f and constraints g_i with GPR. To achieve this, we use a scalar-valued function in a higher dimensional domain describing both the objective and the constraints proposed by [24] :

$$h(a, i) = \begin{cases} f(a) & \text{if } i = 0, \\ g_i(a) & \text{if } i \in \mathcal{I}_g, \end{cases} \quad (6)$$

with $\mathcal{I}_g = \{1, \dots, q\}$, $\mathcal{I} := \{0, 1, \dots, q\}$, and $i \in \mathcal{I}$.

3.2. Calibrated Confidence Intervals

To avoid failures, we must determine the safety of a given policy before evaluating it. To this end, we must reason about plausible worst-case values of the constraint g_i for a new policy a_n . We use the posterior distribution over constraints given by Eq. (5) to build calibrated confidence intervals, i.e., intervals where function values lie with high probability given the data. For functions fulfilling Assumption 2 and 3, [36; 37] use the GP posterior to construct

¹Assumed to be zero without loss of generality (w.l.o.g).

calibrated confidence intervals which depend on the maximum information gain γ_T (cf., [38]).

$$\gamma_T := \max_{A \subset D: |A|=T} I(y_A; f_A),$$

where $I(y_A; f_A)$ is the mutual information between f and the observations y_A , i.e., the measure of the amount of information y_A contains about f and vice versa.

Theorem 3.1. [37, Thm.2] Let f fulfill Assumptions 2 and 3. Let γ_{n-1} be the information capacity of kernel k and $\beta_n^{1/2} = B\sigma\sqrt{2(\gamma_{n-1} + 1 + \ln(1/\delta))}$. Then, for all $a \in \mathcal{A}$ and iterations $n \geq 1$ jointly with probability at least $1 - \delta$:

$$|\mu_{n-1}(a) - f(a)| \leq \beta_n^{1/2} \sigma_{n-1}(a). \quad (7)$$

3.3. SAFEOPT

SAFEOPT [24] is a sample-efficient algorithm for black-box constrained optimization problems that guarantees constraint satisfaction, i.e., safety, for all the iterates with high probability. Thus, it can serve as a method for safe exploration in policy search of dynamical systems. SAFEOPT guarantees safety by limiting its evaluations to a set of provably safe inputs. This safe set relies on calibrated monotonic confidence intervals based on Theorem 3.1: $l_n(a, i) = \max(l_{n-1}(a, i), \mu_{n-1}(a, i) - \beta_n^{1/2} \sigma_{n-1}(a, i))$, with $l_0(a, i) = 0$ for all $a \in S_0$, $i \in \mathcal{I}_g$ and $-\infty$ otherwise, $u_n(a, i) = \min(u_{n-1}(a, i), \mu_{n-1}(a, i) + \beta_n^{1/2} \sigma_{n-1}(a, i))$ with $u_0(a, i) = \infty$ for all $a \in \mathcal{A}, i \in \mathcal{I}$. Given a set of provably safe parameters S_{n-1} , SAFEOPT infers the safety of parameters nearby by combining the confidence intervals with the Lipschitz continuity of the constraints:

$$S_n := \bigcap_{i \in \mathcal{I}_g} \bigcup_{a' \in S_{n-1}} \{a \in \mathcal{A} \mid l_n(a', i) - L_a \|a - a'\| \geq 0\}, \quad (8)$$

with L_a the Lipschitz constant of $f(a)$, $g_i(a)$. SAFEOPT explores the safe set by evaluating points that could optimistically expand it, known as expanders (\mathcal{G}_n see Definition 7 in Appendix C). By evaluating potential maximizers (\mathcal{M}_n see Definition 8 in Appendix C) it guarantees convergence to an approximately optimal solution within the largest safe reach-

able set. Due to the local expansion of the safe set (see Eq. (8)), this set of points belongs to the safe area connected to the safe initialization. Thus, in the case of disconnected safe regions, the optimum discovered by SAFEOPT may be a local one (see Fig. 1).

3.4. GOSAFE

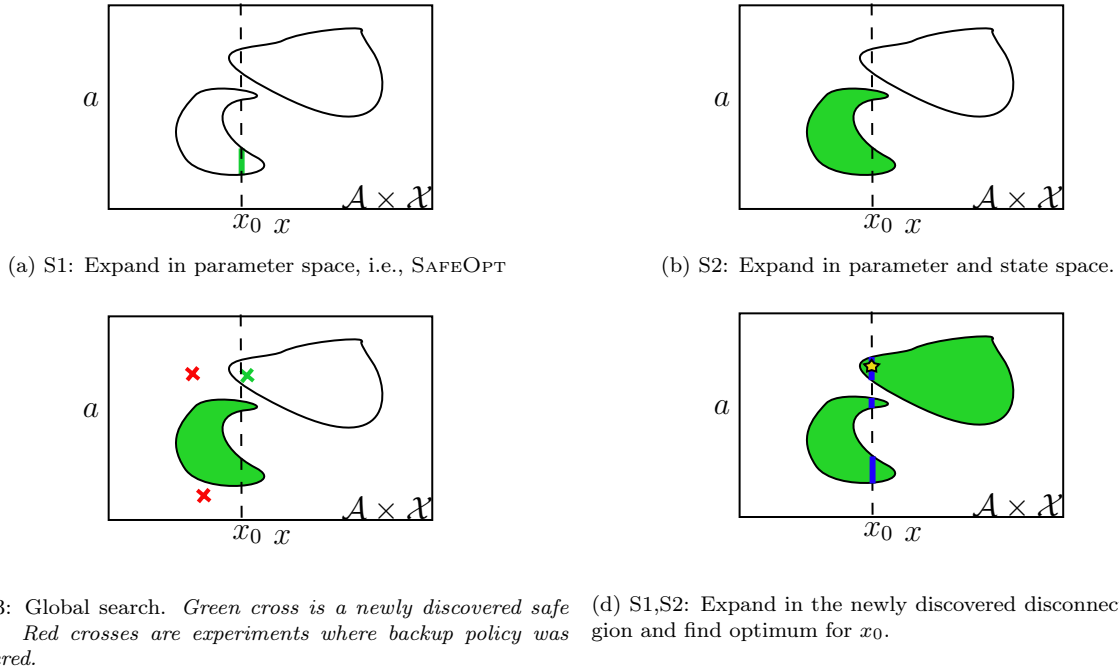


Figure 3: Illustration of GOSAFE steps. *The polygons show the safe set. The green region is the current estimate of the safe set and the golden star the optimum found by GOSAFE.*

GOSAFE [29] is an extension of SAFEOPT, which can discover disconnected safe sets while retaining high probability safety guarantees. To this end, GOSAFE performs a global search, i.e., evaluates potentially unsafe parameters. To preserve safety during global search, it monitors the system state and triggers a safe backup policy if necessary. Thus, it must learn safe backup policies for different states from experiments. Therefore, GOSAFE extends the definition of the safe set to the parameter *and* state space. In particular, it defines S_n as a subset of $\mathcal{A} \times \mathcal{X}_\mu$, where \mathcal{X}_μ is a discretization of the continuous state space \mathcal{X} (see Definitions 9 and 10 in Appendix C). This allows it to learn safe backup policies for different states \tilde{x}_0 by inferring the safety of tuples $(a, \tilde{x}_0) \in \mathcal{A} \times \mathcal{X}_\mu$. Based on this, GOSAFE repeatedly performs the following steps:

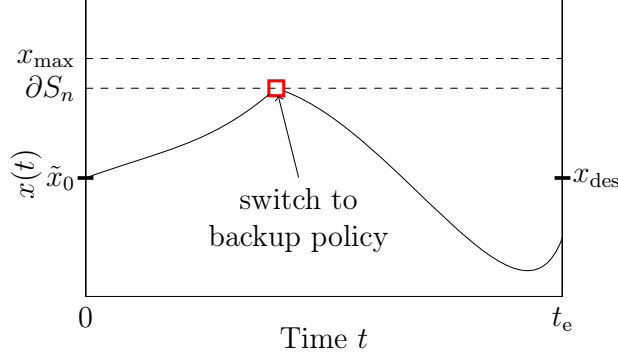


Figure 4: Illustration of when GOSAFE recommends switching to a backup policy. We continuously monitor the state $x(t)$ during the experiment and in case the state hits the border of the set of states for which we know safe backup policies, we switch to the backup policy and avoid constraint violation. Here x_{\max} is defined as $\bar{g}(x_{\max}) = 0$.

S1: Safe exploration in parameter space for the nominal initial condition (equivalent to SAFEOPT) until convergence to the local optimum in the connected safe region (cf. Fig. 3a).

S2: Safe exploration in parameter and state space until there are no more (a, x'_0) tuples that it can safely explore (cf. Fig. 3b). This enables learning of safe backup parameters a for different states \tilde{x}'_0 .

S3: Global evaluation of potentially unsafe policies from a state \tilde{x}_0 for which we know safe backup policies. During the experiment, GOSAFE monitors the rollout and triggers a backup policy if the system reaches a state on the boundary of the safe set, ∂S_n (see Fig. 4). If no backup policy is triggered during the experiment, the parameter is added to the safe set (cf. Fig. 3c).

GOSAFE repeats these steps until the safely reachable part of the domain is fully explored (cf., Fig. 3d) and converges to the safe global optimum under mild conditions.

3.5. Drawbacks of GOSAFE

Despite its successes with simple dynamical systems, GOSAFE presents several shortcomings that hinder its scalability and therefore make its application to complex, real-world settings impossible.

Sample efficiency: GOSAFE fully expands the safe set in $\mathcal{A} \times \mathcal{X}_\mu$. Unfortunately, full safe exploration may require a number of experiments that is exponential in the dimension

of the domain [24; 29], which limits GOSAFE to simple hardware systems, where \mathcal{X}_μ is low-dimensional.

Boundary condition: To preserve safety in **S3**, GOSAFE constantly evaluates a boundary condition, i.e., checks if $x(t) \in \partial S_n$. This has to be done online, which requires it to be fast to evaluate, this is not the case for high-dimensional systems. Additionally, this condition is defined in continuous time, whereas, in practice, we receive discrete time state measurements. To provide practical safety guarantees, this discrepancy is crucial: while $x(t)$ may lie in the interior of the safe set, i.e., $x(t) \in S_n \setminus \partial S_n$, the next state $x(t+\Delta t)$ might be unsafe, $x(t+\Delta t) \notin S_n$. GOSAFE addresses this heuristically.

System reset: During **S2**, GOSAFE needs to reset the system to an arbitrary safe initial condition \tilde{x}_0 , which is challenging even under appropriate *controllability* assumptions [39] because the dynamics model is not known.

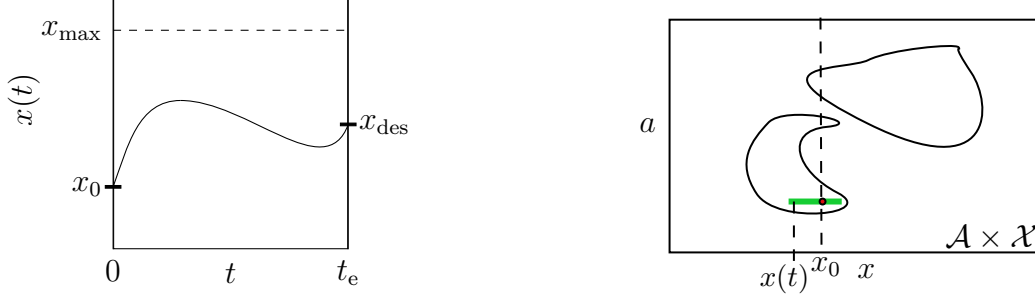
\mathcal{X} discretization: To define the safe set in its extended domain, GOSAFE must discretize the state space, which raises memory and computational concerns when optimizing the acquisition function, updating the safe set, and evaluating the boundary condition.

4. GOSAFE_{OPT}

In this section, we present our novel algorithm, GOSAFE_{OPT}, which retains the sample efficiency of SAFE_{OPT} and the global exploration of GOSAFE to safely discover globally optimal policies for dynamical systems. To the best of our knowledge, GOSAFE_{OPT} is the first algorithm that can globally search for optimal policies, guarantee safety during exploration, and is applicable to complex hardware systems. We describe GOSAFE_{OPT} in detail in Section 4.1 and its safety and optimality guarantees in Section 4.2.

4.1. The algorithm

GOSAFE_{OPT} consists of two alternating stages, local safe exploration (**LSE**) and global exploration (**GE**). In **LSE**, we explore the safe portion of the parameter space connected to our current estimate of the safe set. This step has three main purposes: (i) locally expanding the safe set, (ii) learning about potential optima, and, as a by-product, (iii) learning backup policies for each state we visit during the experiments. When the exploration of the currently



(a) Evolution of the state $x(t)$ under a safe policy. Here x_{\max} is defined as $\bar{g}(x_{\max}) = 0$.

(b) Safe set learned after the experiment. Since all the states visited during the experiment are safe, we can expand the safe set horizontally. This is in contrast to GoSAFE's **S1** where safety of only the initial state x_0 is inferred.

Figure 5: Illustration of the safe set (in green) learned when utilizing the Markov property.

known safe region is complete, i.e., when there is no more relevant information that we can gain by experimenting with provably safe policies, we perform a **GE** step. During **GE**, we evaluate potentially unsafe policies in the hope of identifying new, disconnected safe regions. The safety of this step is guaranteed by triggering the backup policies learned during **LSE** whenever necessary. If a new disconnected safe region is identified, we switch to a **LSE** step. Otherwise, GoSAFE_{OPT} terminates and recommends the optimum from within the safe region with ϵ -precision (see Eq. (A.17)).

In the following, we explain the **LSE** and **GE** stages in more detail and provide their pseudocode in Algorithms 1 and 2, respectively. Algorithm 4 presents the pseudocode for the full GoSAFE_{OPT} algorithm.

4.1.1. Local safe exploration

During **LSE**, we restrict our evaluations to provably safe policies, i.e., policies in the safe set, which is initialized with the safe seed from Assumption 1 and is updated recursively according to Eq. (8) (line 4 in Algorithm 1). To fulfill objectives (i) and (ii) above, we focus our evaluations on two relevant subsets of the safe set introduced in [25]: the maximizers (\mathcal{M}_n), i.e., parameters that are plausibly optimal, and the expanders (\mathcal{G}_n), i.e., parameters that, if evaluated, could optimistically enlarge the safe set. For their formal definitions, see [25] or Appendix C. During **LSE**, we evaluate the most uncertain policy among the expanders

Algorithm 1 LSE

Input: $S, \mathcal{B}, \mathcal{D}$

- 1: Recommend parameter a_n with Eq. (9)
- 2: Collect $\mathcal{R} = \{a_n, x(k)\}_{k \in \mathbb{N}}$ and $h(a_n, i) + \varepsilon_n$
- 3: $\mathcal{B} = \mathcal{B} \cup \mathcal{R}$, $\mathcal{D} = \mathcal{D} \cup \{a_n, h(a_n, i) + \varepsilon\}$
- 4: Update safe set $S, \mathcal{G}, \mathcal{M}$ //Eq. (8), Appendix C Definitions 7 and 8

Return: $S, \mathcal{B}, \mathcal{D}$

and the maximizers:

$$a_n = \arg \max_{a \in \mathcal{G}_n \cup \mathcal{M}_n} \max_{i \in \mathcal{I}} w_n(a, i), \quad (9)$$

where $w_n(a, i) = u_n(a, i) - l_n(a, i)$.

As a by-product of these experiments, GOSAFEOPTE learns backup policies for all the states visited during these rollouts by leveraging the Markov property, thus fulfilling objective (iii) above. Intuitively, for any state $x(t)$ visited when deploying a safe policy a starting from x_0 , we know that the sub-trajectory $\{x(\tau')\}_{\tau' \geq t}$ is also safe because of Assumption 4. Moreover, this sub-trajectory is safe regardless of how we reach $x(t)$ since the state is Markovian. Thus, a is a valid backup policy for $x(t)$. This intuition is formalized in Proposition 1 in the appendix.

This means we *learn about backup policies for multiple states during a single LSE experiment* (cf. Fig. 5). To make them available during **GE**, we introduce the set of backups \mathcal{B}_n . After running an experiment with policy a , we collect all the discrete state measurements in the rollout $\mathcal{R} := \{a, x(k)\}_{k \in \mathbb{N}}$ and add it to the set of backups, $\mathcal{B}_{n+1} = \mathcal{B}_n \cup \mathcal{R}$ (see Algorithm 1 line 3).

We perform **LSE** until the connected safe set is fully explored. Intuitively, this happens when we have learned our constraint function with high precision, i.e., when the uncertainty among the expanders and maximizers is less than ϵ , and yet the safe set does not expand any further

$$\max_{a \in \mathcal{G}_{n-1} \cup \mathcal{M}_{n-1}} \max_{i \in \mathcal{I}} w_{n-1}(a, i) < \epsilon \wedge S_{n-1} = S_n. \quad (10)$$

4.1.2. Global exploration

While **LSE** can be proven to find an ϵ -approximate optimum within a connected safe region, other disconnected safe regions may contain better optima, see Fig. 1. **GE** aims at discovering new, disconnected safe regions by evaluating the most uncertain parameters outside of the safe set, i.e., $a \in \mathcal{A} \setminus S_n$. Crucially, this a is not guaranteed to be safe. Therefore, we monitor the state evolution during the experiment and trigger a backup policy, learned during **LSE**, if there is an imminent danger of violating safety constraints (see lines 3 to 9 in Algorithm 2), which is detected by evaluating a boundary condition. This boundary condition is crucial as it influences the safety and the computational feasibility of **GE** and will be discussed later in detail.

If a backup policy is triggered when evaluating the parameter a , we mark the experiment as failed. To avoid repeating the same experiment, we store a and the state x_{Fail} where we intervened in \mathcal{E} and $\mathcal{X}_{\text{Fail}}$, respectively (see line 9 in Algorithm 2). Thus, during **GE**, we employ the acquisition function

$$a_n = \arg \max_{a \in \mathcal{A} \setminus (S_n \cup \mathcal{E})} \max_{i \in \mathcal{I}_g} w_n(a, i), \quad (11)$$

which suggests the most uncertain parameter that is not provably safe but that has not been shown to trigger a backup policy. If the experiment was run without triggering a backup, we know that a is safe. Therefore, we add the rollout \mathcal{R} collected during the experiment to our set of backups \mathcal{B}_n , i.e., $\mathcal{B}_{n+1} = \mathcal{B}_n \cup \mathcal{R}$, add the parameter a to our safe set, and update its lower bound, i.e., $l_n(a, i) = 0, \forall i \in \mathcal{I}_g$ (see lines 12 and 13 in Algorithm 2). In this case, we switch to **LSE** to explore the newly discovered safe area.

If all the parameters in $\mathcal{A} \setminus (S_n \cup \mathcal{E})$ trigger a backup policy, there are no further safe areas we can discover and **GE** has converged.

Boundary Condition

The boundary condition is evaluated *online* whenever we receive a state measurement to determine whether to trigger a backup policy. Ideally, it must (i) guarantee safety, (ii) be fast to evaluate even for complex dynamical systems, and (iii) incorporate discrete time measurements of the state. To address (iii), we make the following assumption,

Algorithm 2 GE

Input: $S, C, \mathcal{B}, \mathcal{D}, \mathcal{E}, \mathcal{X}_{\text{Fail}}$

- 1: Recommend global parameter a_n with Eq. (11)
- 2: $a = a_n, x_{\text{Fail}} = \emptyset, \text{Boundary} = \text{False}$
- 3: **while** Experiment not finished **do** //Rollout policy
- 4: $x(k) = x_0 + \int_{t=0}^{kT} z(x(t), \pi(x(t); a)) dt$
- 5: **if** Not Boundary **then** //Not at boundary yet
- 6: Boundary, $a_s^* = \text{Boundary Condition}(x(t), \mathcal{B})$
- 7: **if** Boundary **then** //Trigger backup policy
- 8: $a = a_s^*, x_{\text{Fail}} = x(k)$
- 9: $\mathcal{E} = \mathcal{E} \cup a_n, \mathcal{X}_{\text{Fail}} = \mathcal{X}_{\text{Fail}} \cup x_{\text{Fail}}$ //update fail sets
- 10: Collect $\mathcal{R} = \{a_n, x(k)\}_{k \in \mathbb{N}}$, and $h(a_n, i) + \varepsilon_n$
- 11: **if** Not Boundary **then** //Successful global search
- 12: $\mathcal{B} = \mathcal{B} \cup \mathcal{R}$ and $\mathcal{D} = \mathcal{D} \cup \{a_n, h(a_n, i) + \varepsilon_n\}$
- 13: $S = S \cup a, C(a, i) = C(a, i) \cap [0, \infty]$ for all $i \in \mathcal{I}_g$.

Return: $S, C, \mathcal{B}, \mathcal{D}, \mathcal{E}, \mathcal{X}_{\text{Fail}}$

Algorithm 3 Evaluation of the Boundary Condition

Input: x, \mathcal{B}_n

- 1: Boundary = $\forall (a_s, x_s) \in \mathcal{B}_n, \exists i \in \mathcal{I}_g, l_n(a_s, i) - L_x(\|x - x_s\| + \Xi) < 0$
 - 2: **if** Boundary **then** //If at boundary, get backup parameter
 - 3: Calculate a_s^* (Eq. (12))
- return:**
- Boundary,
- a_s^*
-

Assumption 5. For any $x(t)$ and $\rho \in [0, 1]$, the distance to $x(t + \rho\Delta t)$ induced by any action is bounded by a known constant Ξ , that is,

$$\|x(t + \rho\Delta t) - x(t)\| \leq \Xi.$$

Typically, Ξ is not known. However, for many real-world systems, the sampling frequencies are high compared to their time constants, and a conservative yet practical value for Ξ can be obtained from domain knowledge.

Given Assumption 5, our boundary condition leverages the Lipschitz continuity of the constraint to guarantee with high probability that the backup policy is triggered in time to preserve safety, i.e., to fulfill requirement (i). In particular, when we are in $x(t)$, we check if there is a point (a_s, x_s) in our set of backups such that x_s is sufficiently close to $x(t)$ to

guarantee that a_s can steer the system back to safety for any state we may reach in the next time step.

Definition 2. We trigger a backup policy at x if there is not a point in our set of backups $(a_s, x_s) \in \mathcal{B}_n$ such that $l_n(a_s, i) \geq L_x (\|x - x_s\| + \Xi)$ for all $i \in \mathcal{I}_g$. In this case, we propose the backup parameter a_s^*

$$a_s^* = \max_{\{a_s \in \mathcal{A} | \exists x_s \in \mathcal{X}; (a_s, x_s) \in \mathcal{B}_n\}} \min_{i \in \mathcal{I}_g} l_n(a_s, i) - L_x \|x - x_s\|. \quad (12)$$

Since we already calculate $l_n(a_s, i)$ for all $i \in \mathcal{I}_g$ and $a_s \in S_n$ *offline* to update the safe set (see Eq. (8)), we only need to evaluate $\|x - x_s\|$ *online*, which is computationally cheap. Thereby, it satisfies requirement (ii) and enables the application of our algorithm to complex systems with high sampling frequencies. The boundary condition is summarized in Algorithm 3.

4.1.3. Bringing **LSE** and **GE** together

GOSAFEOPT involves two alternating stages, **LSE** and **GE**. In **LSE**, we fully explore the connected safe region and learn backup policies by leveraging the Markov property (see line 7 in Algorithm 4). Then, we perform **GE** to seek other safe parameters globally. If a new parameter is discovered during **GE**, **LSE** is repeated.

Whenever we execute **LSE**, we learn new backup policies, which makes the boundary condition less restrictive. Hence, it may happen that a parameter a that triggered a backup policy during a previous **GE** step, i.e., $a \in \mathcal{E}$, would not do so after a new **LSE** step is completed. Thus, after learning new backup policies during **LSE**, we re-evaluate the boundary condition for all the states where it was previously triggered, i.e., the states in $\mathcal{X}_{\text{Fail}}$ (line 3 to 5 in Algorithm 4), and update \mathcal{E} and $\mathcal{X}_{\text{Fail}}$ accordingly.

GOSAFEOPT converges when the safe set cannot be expanded any further during **LSE** or **GE** (see line 2 in Algorithm 4). After this, GOSAFEOPT recommends the policy $a^* = \arg \max_{a \in S_n} l_n(a, 0)$.

Algorithm 4 GOSAFE_{OPT}

Input: Domain \mathcal{A} , $k(\cdot, \cdot)$, S_0 , C_0 , \mathcal{D}_0 , κ , η

```
1: Initialize GP  $h(a, i)$ ,  $\mathcal{E} = \emptyset$ ,  $\mathcal{X}_{\text{Fail}} = \emptyset$ ,  $B_0 = \{(a, x_0) \mid a \in S_0\}$ 
2: while  $S_n$  expanding or  $\mathcal{A} \setminus (S_n \cup \mathcal{E}) \neq \emptyset$  do
3:   for  $x \in \mathcal{X}_{\text{Fail}}$  do                                     //reevaluate fail sets
4:     if Not Boundary Condition( $x, \mathcal{B}_n$ ) then                 //Algorithm 3
5:        $\mathcal{E} = \mathcal{E} \setminus a$ ,  $\mathcal{X}_{\text{Fail}} = \mathcal{X}_{\text{Fail}} \setminus x$  //If  $x$  not at boundary, update fail sets
6:     Update  $C_n(a, i) := [l_n(a, i), u_n(a, i)] \forall a \in \mathcal{A}, i \in \mathcal{I}_g$  //see Section 3.3
7:     if LSE not converged (Eq. (10)) then                       //Perform LSE (Algorithm 1)
8:        $S_{n+1}, \mathcal{B}_{n+1}, \mathcal{D}_{n+1} = \text{LSE}(S_n, \mathcal{B}_n, \mathcal{D}_n)$ 
9:     else                                                         //Perform GE (Algorithm 2)
10:       $S_{n+1}, C_{n+1}, \mathcal{B}_{n+1}, \mathcal{D}_{n+1}, \mathcal{E}, \mathcal{X}_{\text{Fail}} = \text{GE}(S_n, C_n, \mathcal{B}_n, \mathcal{D}_n, \mathcal{E}, \mathcal{X}_{\text{Fail}})$ 
return:  $\arg \max_{a \in S_n} l_n(a, 0)$ 
```

4.1.4. Advantages of GOSAFE_{OPT}

Compared to SAFE_{OPT}, GOSAFE_{OPT} finds better policies due to the discovery of disconnected safe regions during **GE**. Compared to GOSAFE, it is substantially more sample efficient as it learns multiple backup policies per experiment without actively exploring the state space. Moreover, avoiding the active exploration of \mathcal{X} addresses the system reset concerns of GOSAFE and, together with the new boundary condition, removes the need to discretize the state space, which relieves the computational and memory concerns related to this step for high-dimensional systems. In theory, these crucial practical improvements may reduce the probability of finding the safe global optimum, as we show in Section 4.2.2. This is because GOSAFE_{OPT}'s passive discovery of backup policies may learn fewer of them compared to GOSAFE. Therefore, GOSAFE_{OPT} may have a stricter boundary condition than GOSAFE, which lowers its chances of discovering new safe regions. In practice, this is often not a concern as the additional backup policies learned by GOSAFE pertain to states that are unlikely under an optimal policy (see Fig. 6). This intuition is confirmed by our experiments in Section 5. Finally, our new boundary condition is significantly cheaper to evaluate than GOSAFE's and directly incorporates discrete time measurements, which GOSAFE addressed heuristically without any guarantees. This comparison is summarized in Fig. 7.

In summary, this makes GOSAFE_{OPT} the first algorithm for global safe exploration of

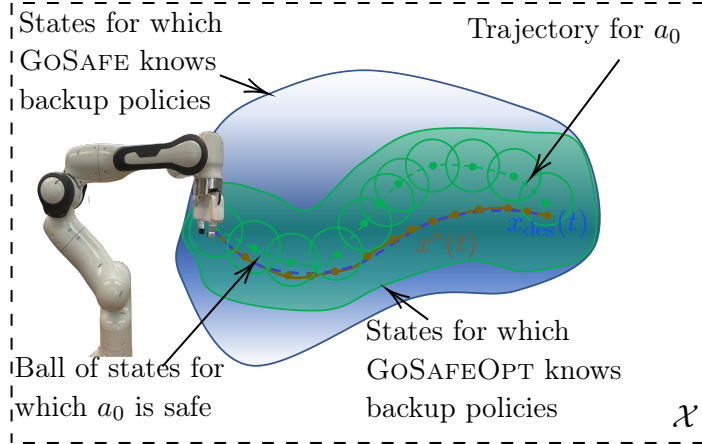


Figure 6: Illustration of GoSAFEOPT compared to GoSAFE. The figure depicts a path following task with desired trajectory $x_{des}(t)$ and the trajectory $x^*(t)$ of the globally optimal parameter. It compares the set of states for which GoSAFE has a backup policy (blue) to ones for which GoSAFEOPT has (green). The gradient of the blue set indicates the likelihood of the states in GoSAFE’s set being visited during any safe experiment starting at x_0 . GoSAFE by actively exploring in the state space can learn backup policies for more states, however some of these states are unlikely to be visited when starting an experiment at our initial condition of interest x_0 . For each state in the trajectory of a_0 , we have a ball of states for which a_0 can be used as a backup parameter. The union of these balls represents the set of states for which a_0 can be used as a safe backup.

complex dynamical systems, to the best of our knowledge.

4.2. Theoretical Results

This section provides safety (Section 4.2.1) and optimality (Section 4.2.2) guarantees for GoSAFEOPT.

4.2.1. Safety Guarantees

The main safety result for our algorithm is that GoSAFEOPT guarantees safety during all experiments.

Theorem 4.1. Let Assumptions 1 – 5 hold and β_n be defined as in Theorem 3.1, GoSAFEOPT guarantees safety with probability at least $1 - \delta$. That is, for all $n \geq 0$ the experiments are safe (see Definition 1).

The proof of this theorem is provided in Appendix A.1. Intuitively, since GoSAFEOPT consists of two alternating search steps (see Section 4.1), we can analyze their safety separately. Concerning the safety of **LSE**, we can leverage the results in [24], which studies it extensively. Therefore, novel to our analysis is the safety of **GE**. Specifically, the boundary con-

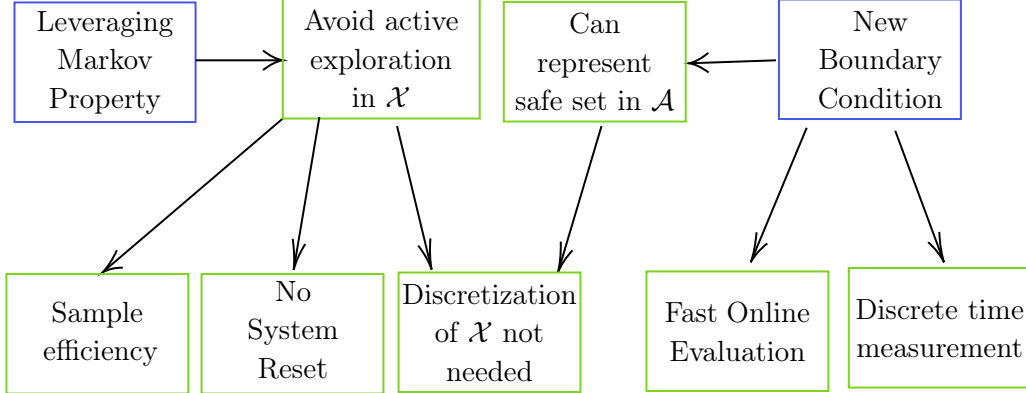


Figure 7: Advantages of GoSAFE OPT. In blue boxes are the two main components of GoSAFE OPT, leveraging the Markov property and the new boundary condition. The arrows indicate the relation between these components and the advantages of GoSAFE OPT over GoSAFE (green boxes).

dition we employ (see Definition 2), which depends on the set of backups we collect by leveraging the Markov property. We show that our proposed boundary condition guarantees with high probability that a backup policy is triggered in time. Therefore, when running experiments during **GE**, we can guarantee that if our boundary condition triggers a backup, we are safe and if it does not, then the experiment was safe, i.e., we discovered a new safe parameter.

4.2.2. Optimality Guarantees

Next, we analyze when GoSAFE OPT can find the safe global optimum a^* , which is the solution to Eq. (2). GoSAFE OPT discovers new safe parameters either during **LSE** or during **GE**. During **LSE**, we explore the connected safe region. For each safe region we explore, we can leverage the results from [24] to prove optimality. Furthermore, due to **GE**, we can discover disconnected safe regions and then repeat **LSE** to explore them. To this end, we define what a discoverable safe set is, i.e., a set of safe parameters that GoSAFE OPT will eventually discover either during **LSE** or during **GE**.

Definition 3. The set $A \subseteq \mathcal{A}$ is discoverable by GoSAFE OPT, if there exists a finite integer \bar{n} such that $A \subseteq S_{\bar{n}}$.

Note, the safe set we can discover during **GE** is a random variable, because it depends on our set of backups \mathcal{B}_n , i.e., the rollouts we collect from experiments and the GP posterior. However, for many practical cases, such as path following or stabilization, typically optimal

or near-optimal policies do not induce erratic trajectories and tend to visit similar states as other safe policies. Therefore, it is often the case in practice, that we do not trigger a backup policy for such parameters and explore the region A where they lie (see Lemma A.16 in Appendix A.2.2). In this case, GOSAFE_{OPT} can find the safe global optimum with ϵ -precision.

Theorem 4.2. Let a^* be the safe global optimum. Further, let Assumptions 1 – 5 hold, β_n be defined as in Theorem 3.1, and assume $a^* \in A^*$, where A^* is a discoverable safe set as defined in Definition 3. Then, there exists a finite integer \bar{n} such that with probability at least $1 - \delta$,

$$f(\hat{a}_{\bar{n}}) \geq f(a^*) - \epsilon, \quad (13)$$

with $\hat{a}_{\bar{n}} = \arg \max_{a \in S_{\bar{n}}} l_{\bar{n}}(a, 0)$.

In practice, GOSAFE_{OPT} tends to find better controllers than SAFE_{OPT}, which converges after **LSE**. However, since it does not actively explore in state space like GOSAFE, GOSAFE might find better parameters. Nonetheless, due to the drawbacks of GOSAFE (see Section 3.5), it cannot be applied to most dynamical systems.

4.3. Practical Modifications

So far, we presented a very practical algorithm for searching globally optimal policies in complex systems that provides safety and optimality guarantees. In practice, we can further improve the sample and computational efficiency by introducing minor modifications. While they hinder our theoretical analysis, they yield well performing results for our evaluation (see Section 5). Below we discuss these modifications.

4.3.1. Fixing Iterations for Each Stage

In Algorithm 4, we perform a global search, i.e., **GE**, after the convergence of **LSE**. Nonetheless, it may be beneficial to run **LSE** for a fixed amount of steps and then switch to **GE**, irrespective of **LSE**'s convergence. This heuristic allows for the early discovery of disconnected safe regions, which may improve sample efficiency and the quality of early solutions. Moreover, this allows to “jump” between different safe regions of the domain that,

even though would be connected if we ran the current **LSE** to convergence, are currently disconnected. These “jumps” may further improve sample efficiency and the quality of early solutions. To this end, we apply the following heuristic scheme.

1. Run **LSE** for n_{LSE} steps.
2. Run **GE** for n_{GE} steps or till we have discovered new safe parameters.
3. If a new region was discovered during **GE**, return to 1. Else, return to 1. but with reduced n_{LSE} .

4.3.2. Update Boundary Condition

If required, the boundary condition can be further modified to reduce computation time. Consider the interior and marginal sets defined below.

Definition 4. The interior set Ω_I and marginal set Ω_M are defined as

$$\begin{aligned}\Omega_I &= \{x_s \in \mathcal{X} \mid (a, x_s) \in \mathcal{B}_n : \forall i \in \mathcal{I}_g, l_n(a, i) \geq \eta_u\} \\ \Omega_M &= \{x_s \in \mathcal{X} \mid (a, x_s) \in \mathcal{B}_n : \forall i \in \mathcal{I}_g, \eta_l \leq l_n(a, i) < \eta_u\}\end{aligned}$$

with $\eta_l < \eta_u$.

The interior set contains the points in our set of backups \mathcal{B}_n that are safe with a high tolerance η_u , whereas the points in the marginal set are safe with a smaller tolerance η_l . We use those sets to evaluate the updated boundary condition instead of the larger set of backups \mathcal{B}_n that we collect. This further reduces the online computation time.

Definition 5. We trigger a backup policy at x if there is not a point $x_s \in \Omega_I$ such that $\|x - x_s\| \leq d_u$ or there is not a point $x'_s \in \Omega_M$ such that $\|x - x'_s\| \leq d_l$ with $d_l < d_u$. In this case, we propose the backup parameter a_s^*

$$a_s^* = \max_{\{a_s \in \mathcal{A} \mid \exists x_s \in \mathcal{X}; (a_s, x_s) \in \mathcal{B}_n\}} \min_{x_s \in \Omega_I \cup \Omega_M} \|x - x_s\|. \quad (14)$$

Intuitively, for points $(a_s, x_s) \in \mathcal{B}_n$ that are safe with high tolerance, i.e., $x_s \in \Omega_I$, our current state x can be further away (d_u) from x_s and still be safe for the parameter a_s . However, for points $(a'_s, x'_s) \in \mathcal{B}_n$ that are safe with a smaller tolerance, that is $x'_s \in \Omega_M$, we require smaller distances d_l to ensure safety. By leveraging the ideas from the proof of Theorem 4.1 (see Appendix A.1), appropriate relations between η_u, d_u , respectively η_l, d_l , can be derived to guarantee safety.

5. Evaluation

We evaluate GOSAFEOPT in simulated and real-world experiments on a Franka Emika Panda seven degree of freedom (DOF) robot arm² (see Fig. 8). Our results show that GOSAFEOPT can scale to high dimensional tasks and jump to disconnected safe regions while guaranteeing safety. Furthermore, they show that GOSAFEOPT is directly applicable to hardware tasks with high sampling frequencies. More details on the experimental setup such as the rewards and constraint functions are provided in Appendix B. The hyperparameters to reproduce our results are listed in Appendix D.

In all experiments with the robot arm, we solely control the position of the end-effector. To this end, we consider an operational space impedance controller [40] with impedance gain K (see Appendix B).

5.1. Simulation Results

We first evaluate GOSAFEOPT in a simulation environment based on the Mujoco physics engine [41]³.

We fix a position $x_{\text{des}} \in \mathbb{R}^3$ which we would like the robot arm to reach. We determine the impedance gain via a linear-quadratic regulator (LQR) controller for which the Q and R matrices are determined by two parameters $q_c \times r \in [2, 6] \times [-3, 3]$ and a linear model is obtained assuming exact feedback linearization [40] (see Appendix B.1). However, because we do not have a model of the system, we cannot perform exact feedback linearization and

²A video of our hardware experiments and link to code are available:
https://sukhijab.github.io/GoSafeCon/main_project.html

³The URDFs and meshes are taken from <https://github.com/StanfordASL/PandaRobot.jl>

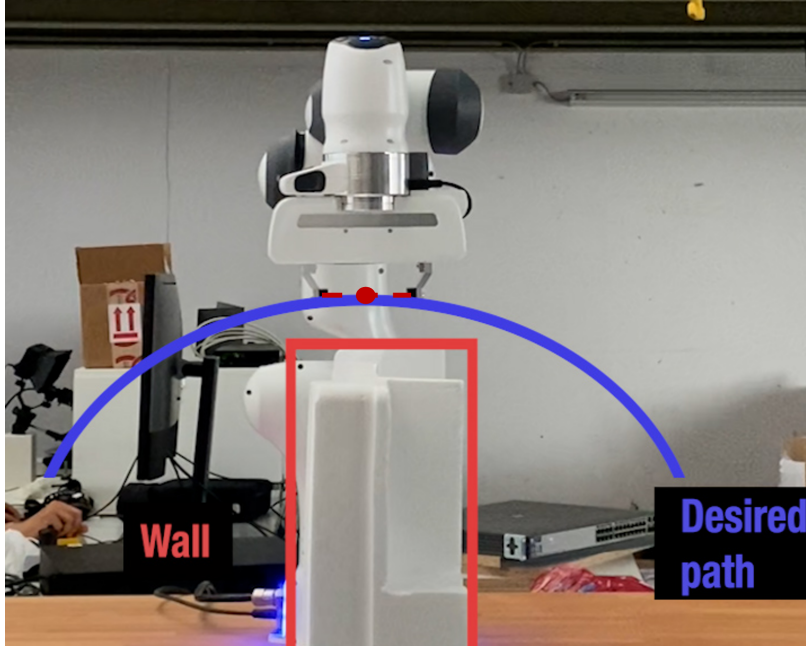
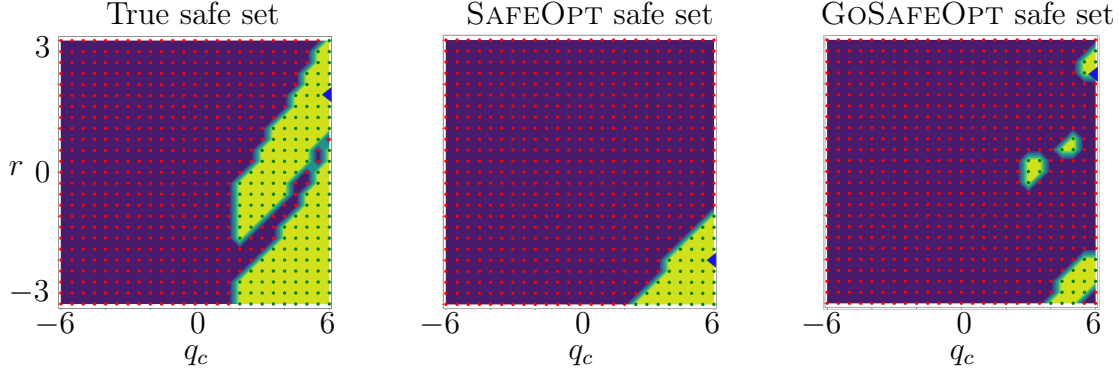


Figure 8: Setup for our evaluation in Section 5. We consider a path following task for the Franka arm. This is a safety-critical problem since deviations from the path (blue) could cause the robot to hit the wall (red box) and incur damage.

there are nonlinearities and imprecisions towards which our policy has to be robust. The state space we consider is six dimensional. Hence, the problem is eight-dimensional (six states, two parameters) and therefore fits into our high dimensional setting. Given that the task is high dimensional, we cannot evaluate the original GOSAFE algorithm for comparison. Therefore, we compare our method to SAFEOPT.

We set the reward function to encourage reaching the target as fast as possible while penalizing large end-effector velocities and control actions. Furthermore, we impose a constraint on the overshoot of the end-effector’s position and the aggressiveness of the impedance gain K (see Appendix B.1 for details). We evaluate our methods over twenty independent runs.

We run a simple grid search to get an estimate of the safe set and the global optimum. Fig. 9 depicts the safe set observed via grid search and the ones discovered by SAFEOPT and GOSAFEOPT after 200 learning iterations. It is visible that there is a disconnected safe region that SAFEOPT is unable to discover and hence is stuck on a local optimum. On the other hand, GOSAFEOPT discovers the disconnected regions and can also jump within connected safe sets. The learning curve of the two methods is depicted in Fig. 11a. Our method performs considerably better than SAFEOPT which is not able to discover a better policy



(a) Contour plot of the safe set (yellow region) (b) Estimated safe set for SAFEOPT at 200 iterations (yellow region). (c) GoSAFEOPT's estimated safe set at 200 iterations (yellow region).

Figure 9: Comparison of the safe set for simulation task between SAFEOPT and GoSAFEOPT. *The yellow regions represent the safe sets. As can be seen, SAFEOPT discovers a connected safe set, whereas GoSAFEOPT discovers many disconnected safe islands. In each figure, the optimum is represented by a blue triangle. The optimum recommended by GoSAFEOPT lies closer to the global optimum from the true safe set, whereas SAFEOPT's recommended optimum is sub-optimal.*

than the initial one after 200 iterations. Furthermore, our method also achieves comparable safety to SAFEOPT (on average 99.9% compared to 100%). We encounter the failures during **LSE** in the second disconnected region where we suspect the constraint function has rough behavior. As the failures are encountered during **LSE**, which corresponds to SAFEOPT, one could also expect similar behavior from SAFEOPT if it were initialized in the upper region.

5.2. Hardware Results

While the simulation results already showcased the general applicability of GoSAFEOPT to high dimensional systems and its ability to discover disconnected safe regions, we now demonstrate that it can also safely optimize policies on real world systems. Specifically, we now apply GoSAFEOPT to the robot arm to find the optimal feedback gain matrix K for a path following task (see the experimental setup in Fig. 8). We model our controller K as

$$K = \text{diag} \left(K_x, K_y, K_z, 2\sqrt{K_x}, 2\sqrt{K_y}, 2\sqrt{K_z} \right),$$

where $K_x = \alpha_x K_{r,x}$ with $K_{r,x} > 0$ a reference value used for Franka's impedance controller and $\alpha_x \in [0, 1.2]$ the parameter we would like to tune (same for y, z). Hence, the parameter space we consider for this task is $[0, 1.2]^3$.

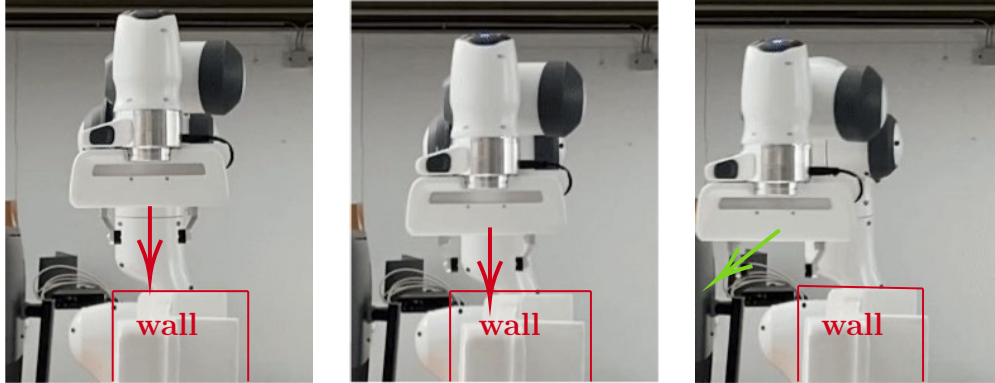


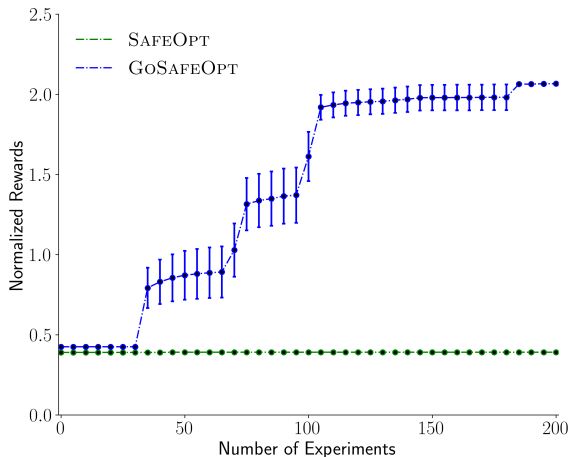
Figure 10: Illustration of triggering the backup policy during **GE**. *During global search, the policy directs the robot towards the wall. A backup policy is automatically triggered by our boundary condition, once the robot gets too close to the wall.*

We require the controller to follow the desired path as accurately as possible. This is especially necessary as the path is very close to the wall as depicted in Fig. 8 and crashing into a wall would likely damage the robot and must be avoided. This simulates a realistic task, where the end-effector is asked to pick up an object on one side of the wall and drop it on the other. We choose our reward function to encourage tracking the desired path as accurately as possible and impose a constraint on the end-effector’s distance from the wall (see Appendix B.2).

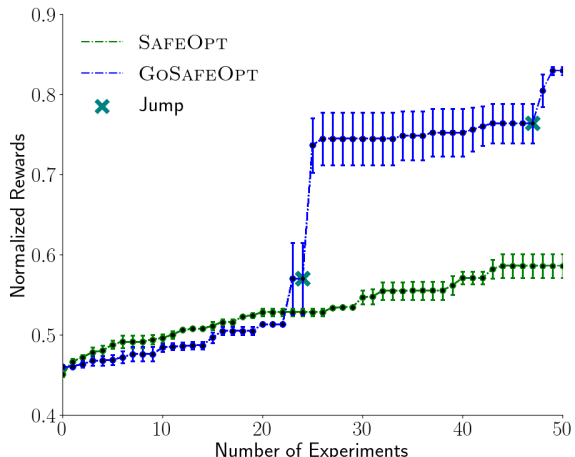
We receive a measurement of the state at 250 Hz and evaluate the boundary condition during **GE** at 100 Hz. As checking the boundary condition only requires calculating the norm between the state x and $x_s \in \Omega_I \cup \Omega_M$ (see Definition 5), it can be evaluated sequentially while maintaining the 250 Hz sampling frequency.

Given the high dimension of the state space, GOSAFE cannot be applied to this task. Hence, we compare our method to SAFEOPTSWARM [32] and run only 50 iterations for each algorithm in three independent runs. We attempt a global search after 20 iterations for GOSAFEOPT.

We choose $a_0 = (0.6, 0.6, 0.6)$ as our initial policy. During our experiments, both GOSAFEOPT and SAFEOPTSWARM provide 100% safety in all three runs. For GOSAFEOPT, this is achieved during **GE** by triggering backup policies in case of danger as illustrated in Fig. 10. Moreover, we see in Fig. 11b that the parameters recommended by GOSAFEOPT



(a) Mean normalized rewards with standard error for SAFEOPT and GoSAFEOPT for the simulation task (20 runs).



(b) Mean normalized rewards with standard error for SAFEOPTSWARM and GoSAFEOPT for the hardware task (3 runs). The approximate location of the jump during \mathbf{GE} is visible and indicated with a cyan cross.

Figure 11: Rewards for GoSAFEOPT and SAFEOPT respectively SAFEOPTSWARM for simulated and real world experiments.

perform considerably better than SAFEOPTSWARM.

6. Conclusion

This work proposes GOSAFEOPT, a novel algorithm for global safe optimization of policies for complex dynamical systems with high-dimensional state spaces ($d > 3$ is considered challenging for existing methods [31]). Global safe search is enabled by learning backup policies and triggering them when the system gets too close to leaving the safe part of the state space. As demonstrated extensively by our experiments, this allows GOSAFEOPT to identify substantially better policies compared to most prior safe exploration methods, such as SAFEOPT, that can only explore locally. Compared to existing methods for safe global search, such as GOSAFE, GOSAFEOPT can handle much more complex and realistic dynamical systems. This is due to a combination of an efficient passive discovery of backup policies that leverages the Markov property of the system and a novel and efficient boundary condition to detect when to trigger a backup policy.

GOSAFE and GOSAFEOPT represent two extreme ends of a continuous spectrum: while GOSAFE exhaustively explores the state space for backup policies, GOSAFEOPT completely forgoes active exploration and leverages the Markov property instead. Clearly, one could

design hybrid algorithms that leverage the Markov property *and* actively explore the state space.

Acknowledgements

We would like to thank Kyrylo Sovailo for helping us with the hardware experiments on the Franka Emika panda arm. The bindings developed (primarily by him) were essential for our hardware experiments.

This project has received funding from the European Research Council (ERC) under the European Union’s Horizon 2020 research and innovation programme grant agreement No 815943, the Swiss National Science Foundation under NCCR Automation, grant agreement 51NF40 180545 and the Microsoft Swiss Joint Research Center.

This work has been funded in parts by the Federal Ministry of Education and Research (BMBF) and the Ministry of Culture and Science of the German State of North Rhine-Westphalia (MKW) under the Excellence Strategy of the Federal Government and the Länder.

References

- [1] R. S. Sutton, A. G. Barto, Reinforcement Learning: An Introduction, 2nd Edition, The MIT Press, 2018.
- [2] V. Mnih, K. Kavukcuoglu, D. Silver, A. Graves, I. Antonoglou, D. Wierstra, M. A. Riedmiller, Playing Atari with deep reinforcement learning, arXiv preprint arXiv:1312.5602 (2013).
- [3] N. Heess, D. TB, S. Sriram, J. Lemmon, J. Merel, G. Wayne, Y. Tassa, T. Erez, Z. Wang, S. M. A. Eslami, M. Riedmiller, D. Silver, Emergence of locomotion behaviours in rich environments, arXiv preprint arXiv:1707.02286 (2017).
- [4] D. Amodei, C. Olah, J. Steinhardt, P. F. Christiano, J. Schulman, D. Mané, Concrete problems in AI safety, arXiv preprint arXiv:1606.06565 (2016).

- [5] A. Ray, J. Achiam, D. Amodei, Benchmarking Safe Exploration in Deep Reinforcement Learning (2019).
- [6] L. Hewing, K. P. Wabersich, M. Menner, M. N. Zeilinger, Learning-based model predictive control: Toward safe learning in control, *Annual Review of Control, Robotics, and Autonomous Systems* 3 (1) (2020) 269–296.
- [7] Y. Kim, R. Allmendinger, M. López-Ibáñez, Safe learning and optimization techniques: Towards a survey of the state of the art, *Trustworthy AI - Integrating Learning, Optimization and Reasoning* (2021).
- [8] L. Brunke, M. Greeff, A. W. Hall, Z. Yuan, S. Zhou, J. Panerati, A. P. Schoellig, Safe learning in robotics: From learning-based control to safe reinforcement learning, *Annual Review of Control, Robotics, and Autonomous Systems* (2021).
- [9] J. Achiam, D. Held, A. Tamar, P. Abbeel, Constrained policy optimization, in: *International Conference on Machine Learning*, 2017, pp. 22–31.
- [10] J. Schulman, S. Levine, P. Abbeel, M. Jordan, P. Moritz, Trust region policy optimization, in: *International Conference on Machine Learning*, 2015, pp. 1889–1897.
- [11] E. Altman, *Constrained Markov Decision Processes*, Chapman and Hall/CRC, 1999.
- [12] Y. Chow, O. Nachum, E. Duenez-Guzman, M. Ghavamzadeh, A Lyapunov-based approach to safe reinforcement learning, in: *Advances in Neural Information Processing Systems*, 2018, p. 8103–8112.
- [13] D. P. Bertsekas, *Dynamic Programming and Optimal Control*, 2nd Edition, Athena Scientific, 2000.
- [14] V. Mnih, K. Kavukcuoglu, D. Silver, A. Graves, I. Antonoglou, D. Wierstra, M. Riedmiller, Playing atari with deep reinforcement learning, *NeurIPS Deep Learning Workshop* (2013).
- [15] K. Srinivasan, B. Eysenbach, S. Ha, J. Tan, C. Finn, Learning to be safe: Deep RL with a safety critic, *arXiv preprint arXiv:2010.14603* (2020).

- [16] J. Mockus, V. Tiesis, A. Zilinskas, The application of Bayesian methods for seeking the extremum, *Towards Global Optimization 2* (117-129) (1978) 2.
- [17] R. Calandra, A. Seyfarth, J. Peters, M. Deisenroth, Bayesian optimization for learning gaits under uncertainty, *Annals of Mathematics and Artificial Intelligence* 76 (2016) 5–23.
- [18] A. Marco, P. Hennig, J. Bohg, S. Schaal, S. Trimpe, Automatic LQR tuning based on Gaussian process global optimization, in: *IEEE International Conference on Robotics and Automation*, 2016, pp. 270–277.
- [19] R. Antonova, A. Rai, C. G. Atkeson, Deep kernels for optimizing locomotion controllers, in: *Conference on Robot Learning*, 2017, pp. 47–56.
- [20] M. Turchetta, A. Krause, S. Trimpe, Robust model-free reinforcement learning with multi-objective Bayesian optimization, in: *IEEE International Conference on Robotics and Automation*, 2020, pp. 10702–10708.
- [21] M. Gelbart, J. Snoek, R. Adams, Bayesian optimization with unknown constraints, *Conference on Uncertainty in Artificial Intelligence* (2014) 250–259.
- [22] J. M. Hernández-Lobato, M. A. Gelbart, R. P. Adams, M. W. Hoffman, Z. Ghahramani, A general framework for constrained Bayesian optimization using information-based search, *The Journal of Machine Learning Research* 17 (1) (2016) 5549–5601.
- [23] F. Berkenkamp, A. P. Schoellig, A. Krause, Safe controller optimization for quadrotors with Gaussian processes, in: *IEEE International Conference on Robotics and Automation*, 2016, pp. 491–496.
- [24] F. Berkenkamp, A. Krause, A. P. Schoellig, Bayesian optimization with safety constraints: safe and automatic parameter tuning in robotics, *Machine Learning* (2021).
- [25] Y. Sui, A. Gotovos, J. Burdick, A. Krause, Safe exploration for optimization with Gaussian processes, in: *International Conference on Machine Learning*, 2015, pp. 997–1005.

- [26] J. Schreiter, D. Nguyen-Tuong, M. Eberts, B. Bischoff, H. Markert, M. Toussaint, Safe exploration for active learning with Gaussian processes, in: *Machine Learning and Knowledge Discovery in Databases*, Springer International Publishing, Cham, 2015, pp. 133–149.
- [27] M. Schillinger, B. Ortelt, B. Hartmann, J. Schreiter, M. Meister, D. Nguyen-Tuong, O. Nelles, Safe active learning of a high pressure fuel supply system, in: *EUROSIM Congress on Modelling and Simulation*, 2018, pp. 286–292.
- [28] C. König, M. Turchetta, J. Lygeros, A. Rupenyan, A. Krause, Safe and efficient model-free adaptive control via Bayesian optimization, arXiv preprint arXiv:2101.07825 (2021). [arXiv:2101.07825](https://arxiv.org/abs/2101.07825).
- [29] D. Baumann, A. Marco, M. Turchetta, S. Trimpe, GoSafe: Globally optimal safe robot learning, in: *IEEE International Conference on Robotics and Automation*, 2021, pp. 4452–4458, Proofs in extended online version: [arXiv 2105.13281](https://arxiv.org/abs/2105.13281).
- [30] E. N. Gryazina, B. T. Polyak, Stability regions in the parameter space: D-decomposition revisited, *Automatica* 42 (1) (2006) 13–26.
- [31] J. Kirschner, M. Mutny, N. Hiller, R. Ischebeck, A. Krause, Adaptive and safe Bayesian optimization in high dimensions via one-dimensional subspaces, in: *International Conference on Machine Learning*, 2019, pp. 3429–3438.
- [32] R. R. Duivenvoorden, F. Berkenkamp, N. Carion, A. Krause, A. P. Schoellig, Constrained Bayesian optimization with particle swarms for safe adaptive controller tuning, *IFAC-PapersOnLine* 50 (1) (2017) 11800–11807, 20th IFAC World Congress.
- [33] B. Schölkopf, A. J. Smola, *Learning with Kernels: Support Vector Machines, Regularization, Optimization, and Beyond*, MIT Press, Cambridge, MA, USA, 2001.
- [34] M. L. Puterman, *Markov decision processes: discrete stochastic dynamic programming*, John Wiley & Sons, 2014.

- [35] C. E. Rasmussen, C. K. I. Williams, Gaussian Processes for Machine Learning (Adaptive Computation and Machine Learning), The MIT Press, 2005.
- [36] N. Srinivas, A. Krause, S. M. Kakade, M. W. Seeger, Information-theoretic regret bounds for Gaussian process optimization in the bandit setting, *IEEE Transactions on Information Theory* 58 (5) (2012) 3250–3265.
- [37] S. R. Chowdhury, A. Gopalan, On kernelized multi-armed bandits, in: *International Conference on Machine Learning*, 2017, pp. 844–853.
- [38] T. M. Cover, J. A. Thomas, *Elements of Information Theory* (Wiley Series in Telecommunications and Signal Processing), Wiley-Interscience, USA, 2006.
- [39] R. E. Kalman, Contributions to the theory of optimal control, *Boletín de la Sociedad Matemática Mexicana* 5 (2) (1960) 102–119.
- [40] B. Siciliano, O. Khatib, *Springer Handbook of Robotics*, 2nd Edition, Springer Publishing Company, Incorporated, 2016.
- [41] E. Todorov, T. Erez, Y. Tassa, Mujoco: A physics engine for model-based control, in: *IEEE/RSJ International Conference on Intelligent Robots and Systems*, 2012, pp. 5026–5033.

A. Theoretical Results

In this section, we provide the proofs for the theoretical results stated in the main body of the paper. In the following, we denote with k discrete time indices and with t continuous ones. This difference is important because, while we obtain state measurements at discrete times, we need to preserve safety at all times. Moreover, similarly to the notation in GOSAFE [29], we denote with $\xi_{(t,x(t),a)} = \{x(t) + \int_t^{t'} z(x(\tau); \pi^a(x(\tau)))d\tau\}_{t' \geq t}$ all the states in the trajectory induced by the policy a starting from $x(t)$ at time t .

A.1. Safety Guarantees

In the following, we prove Theorem 4.1 which gives the safety guarantees for GOSAFEOPT. Since, GOSAFEOPT has two stages, **LSE** and **GE**, we can study their safety separately. For **LSE**, [24] give safety guarantees. Therefore, here we focus on the safety guarantees for **GE**. To this end, we first make a hypothesis on our safe set S_n and confidence bounds $l_n(a, i)$ and $u_n(a, i)$. We leverage this hypothesis to prove that we are safe during **GE** and then we show that it is satisfied for GOSAFEOPT. Particularly, during **LSE**, [24] proves that our hypothesis is fulfilled. Hence, before commencing with **GE**, the safe set and the confidence intervals satisfy it. In the following, we show the updates of the safe sets and the confidence intervals implemented by **GE** also satisfy our hypothesis, which is sufficient to conclude that the hypothesis is satisfied for all $n \geq 0$ (Lemma A.8).

Hypothesis A.1. Let $S_n \neq \emptyset$. The following properties hold for all $i \in \mathcal{I}_g$, $n \geq 0$ with probability at least $1 - \delta$:

$$\forall a \in S_n : g_i(a, x_0) \geq 0, \tag{A.1}$$

$$\forall a \in \mathcal{A} : l_n(a, i) \leq g_i(a, x_0) \leq u_n(a, i). \tag{A.2}$$

Now, we show that, if we trigger a backup policy during an experiment, this experiment is safe with high probability. This proof consists of two parts: showing that we are safe before (Lemma A.4) *and* after (Lemma A.5) we trigger the backup.

First, we show that we guarantee safety before triggering the backup policy. Since the trigger condition is evaluated at discrete times, we start by providing conditions on the values

of the constraint at those discrete times, $g_i(a, x(k))$, which ensure safety in continuous time, i.e., $\bar{g}_i(x(t)) \geq 0$ for all $t \in [k\Delta t, (k+1)\Delta t]$.

Lemma A.2. Let Assumptions 4 and 5 hold and let $k_+ \geq k_- \geq 0$. If for all $k \in [k_-, k_+]$, exists $a_s \in \mathcal{A}$ such that $g_i(a_s, x(k)) \geq L_x \Xi$ for all $i \in \mathcal{I}_g$, then $\bar{g}_i(x(t)) \geq 0$, for all $t \in [k_- \Delta t, (k_+ + 1)\Delta t]$ and $i \in \mathcal{I}_g$.

Proof. By definition of the discrete time step k , $g_i(a_s, x(k)) = g_i(a_s, x(k\Delta t))$.

Consider some $k \geq 0$ and $a_s \in \mathcal{A}$ such that $g_i(a_s, x(k\Delta t)) \geq L_x \Xi$. For any $t \in [k\Delta t, (k+1)\Delta t]$ we have,

$$\begin{aligned} g_i(a_s, x(k\Delta t)) - g_i(a_s, x(t)) &\leq L_x \|x(k\Delta t) - x(t)\| && \text{(Lipschitz continuity)} \\ &\leq L_x \Xi, && \text{(Assumption 5)} \end{aligned}$$

Now, since $g_i(a_s, x(k\Delta t)) \geq L_x \Xi$, we have, for all $t \in [k\Delta t, (k+1)\Delta t]$ and $i \in \mathcal{I}_g$,

$$g_i(a_s, x(t)) \geq g_i(a_s, x(k\Delta t)) - L_x \Xi \geq 0. \quad (\text{A.3})$$

As $g_i(a_s, x(t)) \geq 0$, for all $i \in \mathcal{I}_g$ and $t \in [k\Delta t, (k+1)\Delta t]$, for our choice of constraints (Assumption 4) this implies $\bar{g}_i(x(t)) \geq 0$ for all $i \in \mathcal{I}_g$ and $t \in [k\Delta t, (k+1)\Delta t]$. Therefore, by overlapping the time intervals for all k with $k_- \leq k \leq k_+$, we obtain that for all $t \in [k_- \Delta t, (k_+ + 1)\Delta t]$ and $i \in \mathcal{I}_g$, $\bar{g}_i(x(t)) \geq 0$. \square

Now we have established a condition which guarantees for a given time interval that $\bar{g}_i(x(t)) \geq 0$ for all $i \in \mathcal{I}_g$. Intuitively, the condition says that if there is a safe parameter a_s for $x(k)$, which gives a policy that guarantees safety with high enough tolerance, then we can guarantee safety up until the next time step $k+1$ irrespective of what policy we apply. Hence, the tolerance $L_x \Xi$, takes the worst-case state evolution (according to Assumption 5) over a discrete time step Δt into account.

We collect parameter and state combinations during rollouts in our set of backups \mathcal{B}_n . The intuition here is that for a Markovian system all states visited during a safe experiment are also safe. This is important as it allows GOSAFE OPT to learn backup policies for

multiple states without actively exploring the state space. We formalize this in the following proposition.

Proposition 1. Let Assumption 4 hold. If (a, x_0) is safe, i.e., $\min_{x' \in \xi_{(0, x_0, a)}} \bar{g}_i(x') \geq 0$ for all $i \in \mathcal{I}_g$, then, for all $t_1 \geq 0$, $(a, x(t_1))$ is also safe, that is $\min_{x' \in \xi_{(t_1, x(t_1), a)}} \bar{g}_i(x') \geq 0$ for all $i \in \mathcal{I}_g$.

Proof. The system in Eq. (1) is Markovian, i.e., for any $x(t_1) \in \xi_{(0, x_0, a)}$ and $x(t_2) \in \xi_{(0, x_0, a)}$ with $t_2 > t_1 > 0$,

$$\begin{aligned} x(t_2) &= x_0 + \int_0^{t_2} z(x(t); \pi^a(x(t))) dt \\ &= x_0 + \underbrace{\int_0^{t_1} z(x(t); \pi^a(x(t))) dt}_{x(t_1)} + \int_{t_1}^{t_2} z(x(t); \pi^a(x(t))) dt \\ &= x(t_1) + \int_{t_1}^{t_2} z(x(t); \pi^a(x(t))) dt. \end{aligned}$$

Therefore, we have that a trajectory starting in $x(t_1)$ will always result in the same state evolution, independent of how we arrived at $x(t_1)$. Combining this and Assumption 4 on the nature of the constraint function, we get

$$\begin{aligned} g_i(a, x(t_1)) &= \min_{x' \in \xi_{(t_1, x(t_1), a)}} \bar{g}_i(x') && \text{Assumption 4} \\ &\geq \min_{x' \in \xi_{(0, x_0, a)}} \bar{g}_i(x') && \text{Markov Property} \\ &= g_i(a, x_0) && \text{Assumption 4} \\ &\geq 0. \end{aligned}$$

□

We have now established that our set of backups \mathcal{B}_n consists of safe parameter and state combinations. Nonetheless, in GOSAFE_{OPT}, we do not model the constraint function for each $(a_s, x_s) \in \mathcal{B}_n$, i.e., $g_i(a_s, x_s)$. Specifically, for our boundary condition (Definition 2), we leverage $l_n(a_s, i)$, a lower bound on the function $g_i(a_s, x_0)$. In the following, we show that

$g_i(a_s, x_0)$ itself is a lower bound for all points (a_s, x_s) in \mathcal{B}_n , i.e., $g_i(a_s, x_s) \geq g_i(a_s, x_0)$. This will play a crucial role in showing that we preserve safety whenever we trigger a backup policy.

Corollary A.3. Let Assumption 4 hold. For all points (a_s, x_s) in \mathcal{B}_n , $g_i(a_s, x_s) \geq g_i(a_s, x_0)$ for all $i \in \mathcal{I}_g$.

Proof. Each point (a_s, x_s) in \mathcal{B}_n is collected during experiments (see Algorithm 1 line 3 and Algorithm 2 line 12). Therefore, $x_s \in \xi_{(0, x_0, a_s)}$. The result follows from Proposition 1. \square

Corollary A.3 shows that by considering $l_n(a_s, i)$ in our boundary condition (see Definition 2), we take a conservative lower bound on $g_i(a_s, x_s)$. Crucially, if we can observe not just the rollouts but also the constraint values $g_i(a_s, x_s)$, we could model them with a GP to obtain a potentially less conservative lower bound. However, in our work we only assume that we can measure $g_i(a_s, x_0)$ (Assumption 3).

Proposition 1 and Corollary A.3 give an intuition of how we collect our backup policies and how we leverage them in our boundary condition. Next, we show that if the boundary condition is triggered at a time step k^* , then we are safe up until $k^* \Delta t$, i.e., time of trigger.

Lemma A.4. Let the assumptions from Theorem 4.1 and Hypothesis A.1 hold. If, during **GE**, the boundary condition from Algorithm 3 triggers a backup policy at time step $k^* > 0$, then, for all $t \leq k^* \Delta t$ and $i \in \mathcal{I}_g$, $\bar{g}_i(x(t)) \geq 0$ with probability at least $1 - \delta$.

Proof. Consider $k < k^*$. Since the boundary condition (Algorithm 3) did not trigger a backup policy at k , we have

$$\exists (a_s, x_s) \in \mathcal{B}_n \text{ such that } l_n(a_s, i) \geq L_x (\|x(k) - x_s\| + \Xi), \forall i \in \mathcal{I}_g. \quad (\text{A.4})$$

By Lipschitz continuity of g , we have

$$g_i(a_s, x_s) - g_i(a_s, x(k)) \leq L_x \|x(k) - x_s\|, \quad (\text{A.5})$$

which implies

$$\begin{aligned}
g_i(a_s, x(k)) &\geq g_i(a_s, x_s) - L_x \|x(k) - x_s\| \\
&\geq g_i(a_s, x_0) - L_x \|x(k) - x_s\| && \text{Corollary A.3} \\
&\geq l_n(a_s, i) - L_x \|x(k) - x_s\| && \text{Hypothesis A.1} \\
&\geq L_x \Xi && \text{(A.4)}
\end{aligned}$$

for all $i \in \mathcal{I}_g$ and $k < k^*$. Therefore, we can use Lemma A.2 to prove the claim by choosing $k_- = 0$ and $k_+ = k^* - 1$. □

Lemma A.4 shows that up until the time we trigger our boundary condition, we are safe with enough tolerance ($L_x \Xi$) to guarantee safety. In the following, we show that if we trigger a safe backup policy at k^* , we will fulfill our constraints for all times after trigger.

Lemma A.5. Let the assumptions from Theorem 4.1 and Hypothesis A.1 hold. If during a **GE** experiment with parameter $a_{\mathbf{GE}}$ at time step $k^* \geq 0$, our boundary condition triggers the backup policy a_s^* defined as (see Eq. (12))

$$a_s^* = \arg \max_{\{a \in \mathcal{A} \mid \exists x \in \mathcal{X}; (a, x) \in \mathcal{B}_n\}} \min_{i \in \mathcal{I}_g} l_n(a, i) - L_x \|x - x(k^*)\|. \quad (\text{A.6})$$

Then for all $t \geq k^* \Delta t$, $\bar{g}_i(x(t)) \geq 0$ for all $i \in \mathcal{I}_g$ with probability at least $1 - \delta$.

Proof. We want to show that Eq. (A.6) finds a parameter a_s^* such that $g_i(a_s^*, x(k^*)) \geq 0$. For $k^* = 0$, this follows by definition because \mathcal{B}_n consists of safe rollouts (see Algorithm 1 line 3 and Algorithm 2 line 12) and thus, for all parameters a_s in \mathcal{B}_n and $i \in \mathcal{I}_g$, we have $g_i(a_s, x_0) \geq 0$. Therefore, the case $k^* > 0$ is of interest.

Consider some $(a_s, x_s) \in \mathcal{B}_n$. Following the same Lipschitz continuity based arguments

as in Lemma A.4, we have for all $i \in \mathcal{I}_g$, :

$$\begin{aligned}
g_i(a_s, x(k^*)) &\geq l_n(a_s, i) - L_x \|x_s - x(k^*)\| && \text{same as Lemma A.4} \\
&\geq l_n(a_s, i) - L_x (\|x(k^* - 1) - x_s\| + \|x(k^*) - x(k^* - 1)\|) \\
&\geq l_n(a_s, i) - L_x (\|x(k^* - 1) - x_s\| + \Xi) && \text{(Assumption 5)} \\
&\geq 0,
\end{aligned}$$

where last inequality follows from the fact that the boundary condition was not triggered at time step $k^* - 1$ (see Definition 2). Therefore, for the parameter a_s^* recommended by Eq. (A.6), we have:

$$\begin{aligned}
&\max_{\{a \in \mathcal{A} | \exists x \in \mathcal{X}; (a, x) \in \mathcal{B}_n\}} \min_{i \in \mathcal{I}_g} l_n(a, i) - L_x \|x - x(k^*)\| \geq \\
&\max_{\{a \in \mathcal{A} | \exists x \in \mathcal{X}; (a, x) \in \mathcal{B}_n\}} \min_{i \in \mathcal{I}_g} l_n(a_s, i) - L_x (\|x(k^* - 1) - x\| + \Xi) \geq 0.
\end{aligned}$$

Hence, $g_i(a_s^*, x(k^*)) \geq 0$ for all $i \in \mathcal{I}_g$ with probability at least $1 - \delta$, which proves the claim. \square

Lemmas A.4 and A.5 show that, if we trigger a backup policy during **GE**, we can guarantee the safety of the experiment before and after switching to the backup policy, respectively.

Next, we prove that, if the backup policy is not triggered during a **GE** experiment with parameter $a_{\mathbf{GE}}$, then $a_{\mathbf{GE}}$ is safe with high probability.

Lemma A.6. Let the assumptions from Theorem 4.1 and Hypothesis A.1 hold. If, during **GE** with parameter $a_{\mathbf{GE}}$, a backup policy is not triggered by our boundary condition, then $a_{\mathbf{GE}}$ is safe with probability at least $1 - \delta$, that is, $g_i(a_{\mathbf{GE}}, x_0) \geq 0$ for all $i \in \mathcal{I}_g$.

Proof. Assume the experiment was not safe, i.e., there exists a $t \geq 0$, such that for some $i \in \mathcal{I}_g$ $\bar{g}_i(x(t)) < 0$. Consider the time step $k \geq 0$ such that $t \in [k\Delta t, (k+1)\Delta t]$. Since, the boundary condition was not triggered during the whole experiment, it was also not triggered at time step k . This implies that (see Definition 2) there exists a point $(a_s, x_s) \in \mathcal{B}_n$ such that

$$l_n(a_s, i) - L_x (\|x_s - x(k)\| + \Xi) \geq 0, \quad (\text{A.7})$$

for all $i \in \mathcal{I}_g$. Therefore, we have $g_i(a_s, x(k)) \geq L_x \Xi$ (Hypothesis A.1). Hence, from Lemma A.2 we have $\bar{g}_i(x(t)) \geq 0$ for all $i \in \mathcal{I}_g$. This contradicts our assumption that for some $t \geq 0$ and $i \in \mathcal{I}_g$, $\bar{g}_i(x(t)) < 0$. \square

Next, we summarize our results in the following Corollary, which shows the safety of **GE**, irrespective of whether we triggered a backup policy or not.

Corollary A.7. Let the assumptions from Theorem 4.1 and Hypothesis A.1 hold. GOSAFEOPT is safe during **GE**, i.e., for all $t \geq 0$, $\bar{g}_i(x(t)) \geq 0$ for all $i \in \mathcal{I}_g$.

Proof. There are two scenarios that can occur during **GE**.

1. A backup policy is triggered at some time step $k^* \geq 0$.
2. The experiment is completed without triggering a backup policy.

For the first case, Lemma A.5 guarantees that we are safe after triggering the backup policy, and Lemma A.4 guarantees that we are safe before we trigger the backup. Combining these two, we obtain that we are safe for scenario 1. For second scenario, Lemma A.6 guarantees safety. \square

We have now shown that under the assumptions of Theorem 4.1 combined with Hypothesis A.1, we can guarantee that we are safe during **GE**, irrespective of whether we trigger a backup policy or not. Particularly, if a backup policy was not triggered, the parameter we experimented with is safe with high probability. We leverage this result to show that Hypothesis A.1 is satisfied for GOSAFEOPT.

Lemma A.8. Let the assumptions from Theorem 4.1 hold and β_n be defined as in Theorem 3.1. Then, Hypothesis A.1 is satisfied for GOSAFEOPT, that is, with probability at least $1 - \delta$ for all $i \in \mathcal{I}_g$ and $n \geq 0$

$$\forall a \in S_n : g_i(a, x_0) \geq 0, \tag{A.8}$$

$$\forall a \in \mathcal{A} : l_n(a, i) \leq g_i(a, x_0) \leq u_n(a, i). \tag{A.9}$$

Proof. We prove by induction.

Base case $n = 0$: By Assumption 1, we have, for all $a \in S_0$, $g_i(a, x_0) \geq 0$ for all $i \in \mathcal{I}_g$. Moreover, the initialization of the confidence intervals presented in Section 3.3 is as follows: $l_0(a, i) = 0$ if $a \in S_0$ and $-\infty$ otherwise, and $u_0(a, i) = \infty$ for all $a \in \mathcal{A}$. Thus, it follows that $l_0(a, i) \leq g_i(a, x_0) \leq u_0(a, i)$ for all $a \in \mathcal{A}$.

Inductive step: Our induction hypothesis is $l_{n-1}(a, i) \leq g_i(a, x_0) \leq u_{n-1}(a, i)$ and $g_i(a, x_0) \geq 0$ for all $a \in S_{n-1}$ and for all $i \in \mathcal{I}_g$. Based on this, we prove that these relations hold for iteration n .

We start by showing that $l_n(a, i) \leq g_i(a, x_0) \leq u_n(a, i)$ for all $a \in \mathcal{A}$. To this end, we distinguish between the different updates of the two stages of GOSAFE_{OPT}, **LSE** and **GE**. During **LSE**, we define $l_n(a, i)$ and $u_n(a, i)$ as

$$\begin{aligned} l_n(a, i) &= \max(l_{n-1}(a, i), \mu_n(a, i) - \beta_n \sigma_n(a, i)), \\ u_n(a, i) &= \min(u_{n-1}(a, i), \mu_n(a, i) + \beta_n \sigma_n(a, i)). \end{aligned}$$

We know that $g_i(a, x_0) \geq l_{n-1}$ by induction hypothesis and $g_i(a, x_0) \geq \mu_n(a, i) - \beta_n \sigma_n(a, i)$ with probability $1 - \delta$ because of Theorem 3.1. This implies $g_i(a, x_0) \geq l_n$. A similar argument holds for the upper bound.

During **GE**, we update $l_n(a, i)$ if the parameter we evaluate, a , induces a trajectory that does not trigger a backup policy (see Algorithm 2 line 13). For this parameter, the induction hypothesis allows us to use Lemma A.6 to say $g_i(a, x_0) \geq 0$. Therefore, the update of the confidence intervals during **GE** also satisfies Eq. (A.9) for iteration n , thus completing the induction step for the confidence intervals.

As for the confidence intervals, we distinguish between the different updates of the safe set implemented by **LSE** and **GE**. In case of **GE**, we update the safe set by adding the evaluated controller a only if it does not trigger a backup, i.e., $S_n = S_{n-1} \cup \{a\}$. For the same argument above, we know $g_i(a, x_0) \geq 0$ for all $i \in \mathcal{I}_g$. This together with the induction hypothesis means $g_i(a, x_0) \geq 0$ for all $i \in \mathcal{I}_g$ and $a \in S_n$ in case of a **GE** update.

Now we focus on **LSE**. We showed Eq. (A.9) holds for n . Moreover, we know by induction hypothesis $g_i(a, x_0) \geq 0$ for all $a \in S_{n-1}$ and for all $i \in \mathcal{I}_g$ with high probability. The update equation for the safe set (Eq. (8)) gives us for all $a' \in S_n \setminus S_{n-1}$, $\exists a \in S_{n-1}$ such that for all $i \in \mathcal{I}_g$

$$l_n(a, i) - L_a \|a - a'\| \geq 0. \quad (\text{A.10})$$

We show that this is enough to guarantee with high probability that $g_i(a', x_0) \geq 0$. Particularly, due to the Lipschitz continuity of the constraint functions, we have

$$\begin{aligned} g_i(a', x_0) &\geq g_i(a, x_0) - L_a \|a - a'\|, \\ &\geq l_n(a, i) - L_a \|a - a'\| \geq 0. \end{aligned} \quad (\text{Eq. (A.10)})$$

Therefore, $g_i(a', x_0) \geq 0$ for all $i \in \mathcal{I}_g$ and $a \in S_n$ with probability at least $1 - \delta$ also in case of an **LSE** step.

Since, both the *base case* and *inductive step* have been proved as true, by mathematical induction we have that for all $n \geq 0$, S_n satisfies Hypothesis A.1 for GOSAFEOPT. \square

Lemma A.8 proves that Hypothesis A.1 holds for GOSAFEOPT. We also know that under the same assumption as Theorem 4.1 and Hypothesis A.1, we are safe during **GE** (see Corollary A.7). Hence, we can now guarantee safety during **GE**.

Lemma A.9. Let Assumptions from Theorem 4.1 hold and β_n be defined as in Theorem 3.1. Our proposed rollout procedure and boundary condition (Algorithms 2 and 3) guarantee safety during **GE** with probability at least $1 - \delta$.

Proof. Corollary A.7 proves that when assumptions from Theorem 4.1 and Hypothesis A.1 hold, we are safe during **GE** for our choice of β_n . Furthermore, in Lemma A.8 we proved that Hypothesis A.1 is satisfied for GOSAFEOPT. Hence, we can conclude that if the assumptions from Theorem 4.1 hold, we are safe during **GE** at all times. \square

Finally, we prove Theorem 4.1, which guarantees safety for GOSAFEOPT.

Theorem 4.1. Let Assumptions 1 – 5 hold and β_n be defined as in Theorem 3.1, GOSAFEOPT guarantees safety with probability at least $1 - \delta$. That is, for all $n \geq 0$ the experiments are safe (see Definition 1).

Proof. We perform GOSAFEOPT in two stages; **LSE** and **GE**. In Lemma A.8, we proved that for all parameters $a \in S_n$, $g_i(a, x_0) \geq 0$ for all $i \in \mathcal{I}_g$ with probability at least $1 - \delta$. During **LSE** we query parameters from S_n (Eq. (9)). Therefore, the experiments are safe. During **GE**, we also show that the experiments are safe in Lemma A.9. Therefore, we are safe during all stages of GOSAFEOPT. \square

A.2. Optimality Guarantees

In this section we prove Theorem 4.2 which guarantees that the safe global optimum can be found with ϵ -precision if it lies in a discoverable set (see Definition 3). Then, we show in Lemma A.16, that for many practical applications, the region where the safe global optimum lies is discoverable.

A.2.1. Proof of Theorem 4.2

We first define the largest region that **LSE** can safely discover for a given safe initialization S and then we show that, we can find the optimum with ϵ -precision within this region. To this end, we define reachability operator $R_\epsilon^c(S)$ and the fully connected safe region $\bar{R}_\epsilon^c(S)$

$$R_\epsilon^c(S) := S \cup \{a \in \mathcal{A} \mid \exists a' \in S \text{ such that } g_i(a', x_0) - \epsilon - L_a \|a - a'\| \geq 0, \\ \forall i \in \mathcal{I}_g\}, \quad (\text{A.11})$$

$$\bar{R}_\epsilon^c(S) := \lim_{n \rightarrow \infty} (R_\epsilon^c)^n(S). \quad (\text{A.12})$$

The reachability operator $R_\epsilon^c(S)$ contains the parameters we can safely explore if we know our constraint function with ϵ -precision within some safe set of parameters S . Further, $(R_\epsilon^c)^n(S)$ denotes the repeated composition of $R_\epsilon^c(S)$ with itself, and $\bar{R}_\epsilon^c(S)$ its closure. Next, we derive a property for the the reachability operator, that we will leverage to provide optimality guarantees.

Lemma A.10. The following holds for $\bar{R}_\epsilon^c(S)$:

$$\text{Let } A \subseteq S, \text{ if } \bar{R}_\epsilon^c(A) \setminus S \neq \emptyset, \text{ then } R_\epsilon^c(S) \setminus S \neq \emptyset. \quad (\text{A.13})$$

Proof. This lemma is a trivial generalization of [24, Lem. 7.4]. Assume $R_\epsilon^c(S) \setminus S = \emptyset$, we want to show that this implies $\bar{R}_\epsilon^c(A) \setminus S = \emptyset$. By definition $R_\epsilon^c(S) \supseteq S$ and therefore $R_\epsilon^c(S) = S$. Furthermore, because $A \subseteq S$, we have $\bar{R}_\epsilon^c(A) \subseteq \bar{R}_\epsilon^c(S)$ [24, Lem. 7.1]. Thus, we obtain $\bar{R}_\epsilon^c(A) \subseteq \bar{R}_\epsilon^c(S) = S$, which leads to $\bar{R}_\epsilon^c(A) \setminus S = \emptyset$. □

In the following, we prove that our **LSE** convergence criteria (see Eq. (10)) guarantees that for the safe initialization S , we can explore $\bar{R}_\epsilon^c(S)$ during **LSE** in finite time.

Theorem A.11. Let Assumptions 2 and 3 hold, β_n be defined as in Theorem 3.1 and $S \subseteq \mathcal{A}$ be an initial safe seed of parameters, i.e., $g(a, x_0) \geq 0$ for all $a \in S$. Further let n^* be such that (see Eq. (10))

$$\max_{a \in \mathcal{G}_{n^*-1} \cup \mathcal{M}_{n^*-1}} \max_{i \in \mathcal{I}} w_{n^*-1}(a, i) < \epsilon \wedge S_{n^*-1} = S_{n^*}. \quad (\text{A.14})$$

Then, for any $\epsilon > 0$ and $\delta > 0$, we have that n^* is finite and when running **LSE**, the following holds with probability at least $1 - \delta$ for all $n \geq n^*$:

$$\bar{R}_\epsilon^c(S) \subseteq S_n, \quad (\text{A.15})$$

$$f(\hat{a}_n) \geq \max_{a \in \bar{R}_\epsilon^c(S)} f(a) - \epsilon. \quad (\text{A.16})$$

with $\hat{a}_n = \arg \max_{a \in S_n} l_n(a, 0)$.

Proof. We first leverage the result from [24, Thm. 4.1] which provides the following *worst-case* bound on n^*

$$\frac{n^*}{\beta_{n^*} \gamma_{|\mathcal{I}|n^*}} \geq \frac{C_1 (\bar{R}_0^c(S)) + 1}{\epsilon^2}, \quad (\text{A.17})$$

where $C_1 = 8/\log(1 + \sigma^{-2})$ and n^* is the smallest integer that satisfies Eq. (A.17). Hence, we have that n^* is finite.

Next, we prove Eq. (A.15). For the sake of contradiction, assume $\bar{R}_\epsilon^c(S) \setminus S_{n^*} \neq \emptyset$. This implies, $R_\epsilon^c(S_{n^*}) \setminus S_{n^*} \neq \emptyset$ (Lemma A.10 Eq. (A.13)). Therefore, there exists a $a \in \mathcal{A} \setminus S_{n^*}$ such that for some $a' \in S_{n^*} = S_{n^*-1}$ (Eq. (A.14)), we have for all $i \in \mathcal{I}_g$

$$0 \leq g_i(a', x_0) - \epsilon - L_a \|a - a'\|, \quad (\text{A.18})$$

$$\leq u_{n^*-1}(a', i) - L_a \|a - a'\| \geq 0. \quad (\text{Lemma A.8})$$

Therefore, $a' \in \mathcal{G}_{n^*-1}$ (see [24] or Appendix C Definition 7) and accordingly, $w_{n^*-1}(a', i) < \epsilon$. Next, because $w_{n^*-1}(a', i) < \epsilon$, we have for all $i \in \mathcal{I}_g$

$$0 \leq g_i(a', x_0) - \epsilon - L_a \|a - a'\| \leq l_{n^*-1}(a', i) - L_a \|a - a'\|. \quad (\text{A.19})$$

This means $a \in S_{n^*}$ (Eq. (8)), which is a contradiction. Thus, we conclude that $\bar{R}_\epsilon^c(S) \subseteq S_{n^*}$ and because $S_{n^*} \subseteq S_n$ for all $n \geq n^*$ (Lemma A.12), we get $\bar{R}_\epsilon^c(S) \subseteq S_n$.

Now we prove Eq. (A.16). Consider any $n \geq n^*$. Note, $w_{n^*-1}(a', i) < \epsilon$, implies $w_n(a', i) < \epsilon$ (see Algorithm 1 line 4 or Algorithm 2 line 13). For simplicity, we denote the solution of $\arg \max_{a \in \bar{R}_\epsilon^c(S)} f(a)$ as a_S^* .

$$u_n(a_S^*, 0) \geq f(a_S^*) \quad (\text{Lemma A.8})$$

$$\geq f(\hat{a}_n) \quad (\text{by definition of } a_S^*)$$

$$\geq l_n(\hat{a}_n, 0) \quad (\text{Lemma A.8})$$

$$= \max_{a \in S_n} l_n(a, 0). \quad (\text{by definition of } \hat{a}_n)$$

Therefore, a_S^* is a maximizer, i.e., $a_S^* \in \mathcal{M}_n$ (see Appendix C Definition 8) and has uncertainty less than ϵ , that is $w_n(a_S^*, i) < \epsilon$. Now we show that $f(\hat{a}_n) \geq f(a_S^*) - \epsilon$. For the sake of contradiction assume,

$$f(\hat{a}_n) < f(a_S^*) - \epsilon. \quad (\text{A.20})$$

Then we obtain,

$$\begin{aligned}
l_n(a_S^*, 0) &\leq l_n(\hat{a}_n, 0) && \text{(by definition of } \hat{a}_n) \\
&\leq f(\hat{a}_n) && \text{(Lemma A.8)} \\
&< f(a_S^*) - \epsilon && \text{(by Eq. (A.20))} \\
&\leq u_n(a_S^*, 0) - \epsilon && \text{(Lemma A.8)} \\
&\leq u_n(a_S^*, 0) - w_n(a^*, 0) && \text{(because } w_n(a_S^*, 0) \leq \epsilon) \\
&= l_n(a_S^*, 0), && \text{(by definition of } w_n(a_S^*, 0))
\end{aligned}$$

which is a contradiction. Therefore, we have $f(\hat{a}_n) \geq f(a_S^*) - \epsilon$. □

Theorem A.11 states that for a given safe seed S , convergence of **LSE** (Eq. (10)) implies that we have discovered its fully connected safe region $\bar{R}_\epsilon^c(S)$ and recovered the optimum within the region with ϵ -precision.

Based on the previous results, we can show that if the safe global optimum lies in a discoverable set A^* (see Definition 3), then we can find an approximately optimal safe solution. Note, A^* is discoverable if there exists a finite integer n such that $A^* \subseteq S_n$. However, to prove optimality, what we also require is that if $A^* \subseteq S_n$ then $A^* \subseteq S_{n+1}$. Otherwise, we might have the global optimum in our safe set for some iteration n but we may lose it for some $n_1 > n$. **GOSAFE**OPT guarantees that $S_n \subseteq S_{n+1}$ and therefore this cannot happen.

Lemma A.12. Let the assumptions from Theorem 4.1 hold. For any $n \geq 0$, the following property is satisfied for S_n .

$$S_n \subseteq S_{n+1}, \tag{A.21}$$

Proof. The safe set provably increases during **LSE** [24, Lem. 7.1]. During **GE**, the safe set is only updated if a new safe parameter is found. The proposed update also has the non-decreasing property (see Algorithm 2, line 13). Hence, we can conclude that $S_n \subseteq S_{n+1}$. □

Lemma A.12 shows that if the safe global optimum $a^* \in S_n$, then $a^* \in S_{n+1}$. Furthermore,

Theorem A.11 guarantees that in finite iterations \bar{n} we can achieve $w_{\bar{n}}(a^*, i) < \epsilon$ for all $i \in \mathcal{I}$. This is sufficient for us to find the safe global optimum with ϵ -precision.

Theorem 4.2. Let a^* be the safe global optimum. Further, let Assumptions 1 – 5 hold, β_n be defined as in Theorem 3.1, and assume $a^* \in A^*$, where A^* is a discoverable safe set as defined in Definition 3. Then, there exists a finite integer \bar{n} such that with probability at least $1 - \delta$,

$$f(\hat{a}_{\bar{n}}) \geq f(a^*) - \epsilon, \quad (13)$$

with $\hat{a}_{\bar{n}} = \arg \max_{a \in S_{\bar{n}}} l_{\bar{n}}(a, 0)$.

Proof of Theorem 4.2. Let n be the smallest integer such that $A^* \subseteq S_n$ (Definition 3). In GOSAFEOPT we only perform **GE** after exploring the fully connected safe set (see Eq. (10)). Furthermore, if a new safe region is discovered during **GE**, this is again fully explored during **LSE**. Therefore, we explore each safe region till we have uncertainty less than ϵ in the maximizer and expander set (see Eq. (10)). Theorem A.11 shows that we can find the optimum in the safe region with ϵ precision in finite time $\bar{n} \geq n$. Furthermore, from Lemma A.12, we know that $A^* \subseteq S_{\bar{n}}$, which implies that $a^* \in S_{\bar{n}}$. Hence, there exists a finite integer \bar{n} such that

$$f(\hat{a}_{\bar{n}}) \geq f(a^*) - \epsilon, \quad (\text{A.22})$$

with $\hat{a}_{\bar{n}} = \arg \max_{a \in S_{\bar{n}}} l_{\bar{n}}(a, 0)$.

□

A.2.2. Requirements for Discovering Safe Sets with **GE**

In the previous section, we showed that if a region A^* that contains the safe global optimum a^* is discoverable, we can then find optimum with ϵ -precision. In this section, we show that when a new safe parameter a_{GE} is discovered during **GE**, its fully connected safe region, $\bar{R}_{\epsilon}^c(\{a_{\text{GE}}\})$ will be explored. Following that, we show that if for a parameter a_{GE} in $\mathcal{A} \setminus S_n$, we have backup policies for all the states in its trajectory, then a_{GE} will be eventually added to our safe set of parameters. Finally, we conclude this section by showing that for many practical cases, a^* lies in a discoverable safe set.

Lemma A.13. Consider any integer $n \geq 0$. Let S_n be the safe set of parameters explored after n iterations of GOSAFEOPT, β_n be defined as in Theorem 3.1. Consider $A = S_{n+1} \setminus S_n$. If $A \neq \emptyset$, then there exists a finite integer $\bar{n} > n$ such that $\bar{R}_c^\epsilon(A) \cup \bar{R}_c^\epsilon(S_n) \subseteq S_{\bar{n}}$ with probability at least $1 - \delta$.

Proof. Note, if $\bar{R}_c^\epsilon(A) \setminus S_{\bar{n}} = \emptyset$ and $\bar{R}_c^\epsilon(S_n) \setminus S_{\bar{n}} = \emptyset$ then $\bar{R}_c^\epsilon(A) \cup \bar{R}_c^\epsilon(S_n) \subseteq S_{\bar{n}}$. We now show that $\bar{R}_c^\epsilon(A) \setminus S_{\bar{n}} = \emptyset$. Assume that $\bar{R}_c^\epsilon(A) \setminus S_{\bar{n}} \neq \emptyset$. We know that $A \subseteq S_{n+1} \subseteq S_{\bar{n}}$ (Lemma A.12). This implies $R_c^\epsilon(S_{\bar{n}}) \setminus S_{\bar{n}} \neq \emptyset$ (Lemma A.10 A.13). Since $A \neq \emptyset$, the safe set is expanding. For GOSAFEOPT, this can either happen during **LSE** or during **GE** when a new parameter is successfully evaluated, i.e., boundary condition is not triggered. In either case, we perform **LSE** steps till convergence. Let $\bar{n} > n$ be the integer for which we converge during **LSE** (fulfills condition in Eq. (10)):

$$\max_{a \in \mathcal{G}_{\bar{n}-1} \cup \mathcal{M}_{\bar{n}-1}} \max_{i \in \mathcal{I}} w_{\bar{n}-1}(a, i) < \epsilon \wedge S_{\bar{n}-1} = S_{\bar{n}}. \quad (\text{A.23})$$

From Theorem A.11, we know that \bar{n} is finite. Consider $a \in R_c^\epsilon(S_{\bar{n}}) \setminus S_{\bar{n}}$. Then we have that there exists $a' \in S_{\bar{n}}$ such that $0 \leq g_i(a', x_0) - \epsilon - L_a \|a - a'\|$ (see (A.11)). Furthermore, because $S_{\bar{n}-1} = S_{\bar{n}}$, $a' \in S_{\bar{n}-1}$. Hence, we also have $0 \leq u_{\bar{n}-1}(a, i) - L_a \|a - a'\|$, which implies that, $a' \in \mathcal{G}_{\bar{n}-1}$ (Appendix C Definition 7) and therefore, $w_{\bar{n}-1}(a', i) < \epsilon$. This implies that $0 \leq l_{\bar{n}-1}(a', i) - L_a \|a - a'\|$. Therefore, according to Eq. (8), $a \in S_{\bar{n}}$, which is a contradiction. Hence, $\bar{R}_c^\epsilon(A) \setminus S_{\bar{n}} = \emptyset$. We can proceed similarly to show that $\bar{R}_c^\epsilon(S_n) \setminus S_{\bar{n}} = \emptyset$. Since, we have $\bar{R}_c^\epsilon(A) \setminus S_{\bar{n}} = \emptyset$ and $\bar{R}_c^\epsilon(S_n) \setminus S_{\bar{n}} = \emptyset$, we can conclude that $\bar{R}_c^\epsilon(A) \cup \bar{R}_c^\epsilon(S_n) \subseteq S_{\bar{n}}$. \square

In Lemma A.13 we have shown that for every set A that we add to our safe set, we will explore its fully connected safe region in finite time. This is crucial because it allows us to guarantee that when we discover a new region during **GE**, we explore it till convergence. Now, we derive conditions which allow us to explore new regions/parameters during **GE**. To this end, we start by defining a set of safe states $\mathcal{X}_{s,n}$, i.e., the states for which our boundary condition does not trigger a backup policy (c.f., Fig. A.12).

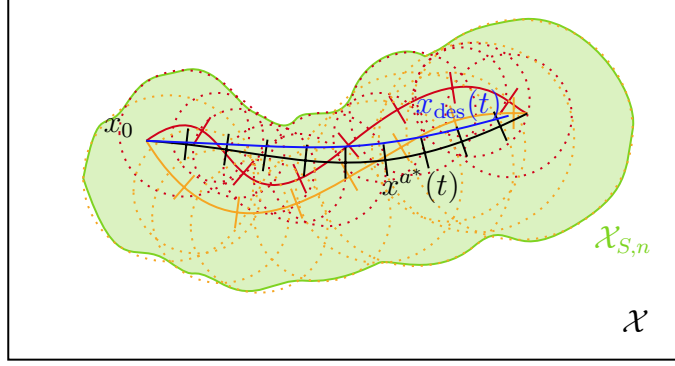


Figure A.12: Illustration of $\mathcal{X}_{S,n}$. In orange and red are safe trajectories starting at x_0 , in blue the desired trajectory, and in black the trajectory of the safe global optimum. For each state we visit during a safe experiment with parameter a , we determine a ball of states for which a can be used as a backup parameter. The union of these balls is $\mathcal{X}_{S,n}$. Since for many practical tasks safe policies visit similar set of states, knowing backup policies for states in $\mathcal{X}_{S,n}$ is sufficient to find the global optimum.

Definition 6. The set of safe states $\mathcal{X}_{s,n}$ is defined as

$$\mathcal{X}_{s,n} := \bigcup_{(a',x') \in \mathcal{B}_n} \left\{ x \in \mathcal{X} \mid \|x' - x\| \leq \frac{1}{L_x} \min_{i \in \mathcal{I}_g} l_n(a', i) - \Xi, \right\}. \quad (\text{A.24})$$

Intuitively, if a trajectory induced by a parameter being evaluated during **GE** lies in $\mathcal{X}_{s,n}$, then the boundary condition will not be triggered for this parameter. As a result, it will be discovered by GOSAFEOPT. Now we will prove that this set of safe states $\mathcal{X}_{s,n}$ is non-decreasing. This is an important property because it tells us that GOSAFEOPT continues to learn backup policies for more and more states.

Lemma A.14. Let the assumptions from Theorem 4.1 hold. For any $n \geq 0$, the following property is satisfied for $\mathcal{X}_{s,n}$.

$$\mathcal{X}_{s,n} \subseteq \mathcal{X}_{s,n+1}. \quad (\text{A.25})$$

Proof. The lower bounds $l_n(a, i)$ are non-decreasing for all $i \in \mathcal{I}$ by definition (see Algorithm 1 line 4 or Algorithm 2 line 13). Additionally, because we continue to add new rollouts to our set of backups, we have $\mathcal{B}_n \subseteq \mathcal{B}_{n+1}$ (see Algorithm 1 line 3 or Algorithm 2 line 12). For each $x \in \mathcal{X}_{s,n}$, there exists $(a_s, x_s) \in \mathcal{B}_n$, such that $l_n(a_s, i) - L_x(\|x - x_s\| + \Xi) \geq 0$ for all $i \in \mathcal{I}_g$. Because $\mathcal{B}_n \subseteq \mathcal{B}_{n+1}$ and $l_{n+1}(a_s, i) \geq l_n(a_s, i)$, $x \in \mathcal{X}_{s,n+1}$. \square

Next, we state conditions for which a parameter $a_{\mathbf{GE}} \in \mathcal{A} \setminus S_n$ will be discovered during

GE, i.e., no backup policy would be triggered during **GE**, in finite time.

Lemma A.15. Consider any $n \geq 0$. Let S_n be the safe set of parameters explored after n iterations of GOSAFEOPT and $a_{\mathbf{GE}}$ a parameter in $\mathcal{A} \setminus S_n$. Further, let the assumptions from Theorem 4.2 hold and β_n be defined as in Theorem 3.1. If for all $k \geq 0$, $x^{a_{\mathbf{GE}}}(k) \in \mathcal{X}_{s,n}$, where, $x^{a_{\mathbf{GE}}}(k)$ represents the state at time step k for the system starting at x_0 with policy $\pi^{a_{\mathbf{GE}}}(\cdot)$, then there exists a finite integer $\bar{n} > n$, such that $a_{\mathbf{GE}} \in S_{\bar{n}}$.

Proof. Assume that there exists no such finite integer $\bar{n} > n$ such that $a_{\mathbf{GE}} \in S_{\bar{n}}$. This would imply that $a_{\mathbf{GE}} \in \mathcal{A} \setminus S_{\bar{n}}$ for all $\bar{n} > n$. Thus, because $a_{\mathbf{GE}}$ will never be a part of our safe set, it will never be evaluated during **LSE**. However, from Theorem A.11 we know that **LSE** will converge in finite number of iterations after which we will perform **GE**. Since, $a_{\mathbf{GE}}$ is not a part of the safe set, it can only be evaluated during **GE**, where parameters outside of the safe regions are queried. The parameter space \mathcal{A} is finite and any parameter that was evaluated unsuccessfully, i.e., boundary condition was triggered, will be added to \mathcal{E} and therefore not evaluated again (see Eq. (11) and Algorithm 2 line 9). This implies that $a_{\mathbf{GE}}$ will be evaluated for some n' with $n < n' < \bar{n}$ (since $S_{n'} \subseteq S_{\bar{n}}$ Lemma A.12). Furthermore, $\mathcal{X}_{s,n} \subseteq \mathcal{X}_{s,n'}$ (Lemma A.14) and therefore for all $k \geq 0$, $x^{a_{\mathbf{GE}}}(k) \in \mathcal{X}_{s,n'}$. If when $a_{\mathbf{GE}}$ is evaluated, the experiment is unsuccessful, i.e., we were to trigger a backup policy, this would imply that for some k and $i \in \mathcal{I}_g$, there is no $(a_s, x_s) \in \mathcal{B}_{n'}$ such that

$$l_{n'}(a, i) \geq L_x(\|x^{a_{\mathbf{GE}}}(k) - x_s\| + \Xi).$$

Thus, we had $x^{a_{\mathbf{GE}}}(k) \notin \mathcal{X}_{s,n'}$, which contradicts our assumption. Therefore, $a_{\mathbf{GE}} \in S_{n'+1} \subseteq S_{\bar{n}}$ (Lemma A.12 A.21), which is a contradiction. Consequently, we have $a_{\mathbf{GE}} \in S_{\bar{n}}$ after a finite number of iterations \bar{n} . \square

Lemma A.15 guarantees that, if for a parameter $a_{\mathbf{GE}}$, its trajectory lies in $\mathcal{X}_{s,n}$, then it will eventually be added to our safe set, either during **LSE** or during **GE**. We utilize this result to provide a condition for a safe region A to be *discoverable* by GOSAFEOPT.

Lemma A.16. Consider any $n \geq 0$. Let Assumptions 1 – 5 hold, β_n be defined as in Theorem 3.1 and let $A \subseteq \mathcal{A}$ be a subset of the parameter space. If there exists $a_{\mathbf{GE}} \in \mathcal{A} \setminus S_n$

such that

- (i) for all $k \geq 0$, $x^{a_{\mathbf{GE}}}(k) \in \mathcal{X}_{s,n}$, where $x^{a_{\mathbf{GE}}}(k)$ is the state visited by system starting at x_0 under the policy $\pi^{a_{\mathbf{GE}}}(\cdot)$ at time step k , and
- (ii) $\bar{R}_\epsilon^c(\{a_{\mathbf{GE}}\}) \supseteq A$,

then the set A is discoverable by GOSAFE_{OPT} with probability at least $1 - \delta$.

Proof. Since, for all $k \geq 0$, $x^{a_{\mathbf{GE}}}(k) \in \mathcal{X}_{s,n}$, there exists a finite integer $\tilde{n} > n$ such that $a_{\mathbf{GE}} \in S_{\tilde{n}}$ (Lemma A.15). Furthermore, from Lemma A.13, it follows that $\bar{R}_\epsilon^c(\{a_{\mathbf{GE}}\})$ will eventually be explored with probability at least $1 - \delta$, i.e., there exists a finite integer $\bar{n} \geq \tilde{n}$ such that $\bar{R}_\epsilon^c(\{a_{\mathbf{GE}}\}) \subseteq S_{\bar{n}}$. Therefore, we have $A \subseteq \bar{R}_\epsilon^c(\{a_{\mathbf{GE}}\}) \subseteq S_{\bar{n}}$, that is, A is discoverable. \square

The condition here is interesting, because for many practical cases it is fulfilled. Crucially, optimal or near-optimal parameters tend to visit similar states as other safe policies. We add rollouts from safe policies to our set of backups \mathcal{B}_n and therefore have backup policies for their trajectories and other trajectories that lie close to them. Therefore, the trajectories of (near-)optimal parameters lie in $\mathcal{X}_{s,n}$ (see Fig. A.12) and in this case, GOSAFE_{OPT} can discover them global safe optimum with ϵ -precision.

B. Additional Information on Experiments

For all our experiments in Section 5, we consider a controller in the operational space. The operational space dynamics of the end-effector are given by [40]

$$u(x(t)) = \Lambda(q)\ddot{s} + \Gamma(q, \dot{q})\dot{s} + \eta(q), \quad (\text{B.1})$$

where s represents the end-effector position, q the joint angles, and $\Lambda(q)$, $\Gamma(q, \dot{q})$, $\eta(q)$ are non linearities representing the mass, Coriolis, and gravity terms, respectively. The state we consider is $x(t) = [s^T(t), \dot{s}^T(t)]^T$

We consider an impedance controller:

$$u(x(t)) = -K \begin{bmatrix} s \\ \dot{s} \end{bmatrix} + \Gamma(q, \dot{q})\dot{s} + \eta(q), \quad (\text{B.2})$$

with K being the feedback gain. The torque τ applied to each of the joints can be calculated via $\tau = J^T u(x(t))$, with J the Jacobian.

Furthermore, the constraints we consider for our experiments are of the form stated in Assumption 4. For our experiments, we can directly measure $g(a, x(k))$, where k denotes discrete time. Therefore, instead of using $l_n(a_s, i)$ for the boundary condition in Section 4.3.2, we take a lower bound over all the tuples in our set of backups, \mathcal{B}_n , i.e., $l_n(a_s, x_s, i)$, which could potentially reduce the conservatism of the boundary condition. However, to determine $l_n(a_s, x_s, i)$, we require a GP which is defined over the parameter and state space, and contains all the points from \mathcal{B}_n . Since, \mathcal{B}_n consists of rollouts from individual experiments, the GP has many points. Therefore, doing inference with it is costly. To this end, we use a subset selection scheme to select a smaller subset of data at random with a probability which is proportional to $\exp(-\min_{i \in \mathcal{I}_g} l_n^2(a, x, i))$. Crucially, we want to retain points that have a small lower bound such that we have low uncertainty around these points. We perform this subset selection once our GP has acquired more than n_{\max} data points. Then, we select a subset of $m < n_{\max}$ points.

Lastly, for the boundary condition from Section 4.3.2, we can define the distance d_u and d_l through the covariance function of our GP. Specifically, for stationary isotropic kernels, we can define the distances d_u (same for d_l) such that $\|x - x'\| \leq d_u \implies k(\|x - x'\|) \geq \kappa_u^2$. This makes the choice of d_u more intuitive since it directly relates to the covariance function of our GP.

B.1. Simulation Results

For the simulation task, we determine the impedance K using an infinite horizon LQR parameterized via

$$Q = \begin{bmatrix} Q_r & 0 \\ 0 & \kappa_d Q_r \end{bmatrix}, Q_r = 10^{q_c} I_3,$$

$$R = 10^{r-2} I_3, A = \begin{bmatrix} 0 & I_3 \\ 0 & 0 \end{bmatrix}, B = \begin{bmatrix} 0 \\ I_3 \end{bmatrix}.$$

The matrices A, B are obtained assuming that we use a feedback linearization controller [40]. However, because we instead use an impedance controller, there are nonlinearities and im-

precisions in our model. The parameters q_c, r, κ_d are tuning parameters we would like to optimize.

The control input we apply is:

$$u(x(t)) = -K \begin{bmatrix} s - s_{\text{des},L}[k] \\ \dot{s} \end{bmatrix} + \Gamma(q, \dot{q})\dot{s} + \eta(q),$$

where $s_{\text{des},L}[k]$ is a discretized target position defined as

$$s_{\text{des},L}[k] = s_0 + \frac{k}{T_{\text{traj}}}(s_{\text{des}} - s_0).$$

Thus, we linearly increase our target, the speed of which is given by $\frac{1}{T_{\text{traj}}}$. The constraint and stage rewards are:

$$\begin{aligned} \bar{g}(x(t)) &= \frac{\|s(t) - s_{\text{des}}\|_2 - \|s(0) - s_{\text{des}}\|_2}{\|s(0) - s_{\text{des}}\|_2} - \alpha, \quad \alpha = 0.08 \\ \mathcal{R}(x(t)) &= -\|s(t) - s_{\text{des}}\|_2^2 / \|s(0) - s_{\text{des}}\|_2^2 \\ &\quad - \frac{1}{25} \|\tanh \dot{s}(t)\|_2^2 - \frac{1}{25} \|\tanh u(x(t))\|_2^2. \end{aligned} \tag{B.3}$$

Hence, the reward encourages reaching the target as fast as possible. However, penalizes large velocities and actions. Furthermore, we want to limit the overshoot in the end-effector's position. Additionally, to encourage fast behaviour, we only sample parameters for which the eigenvalues of $A - BK$ are less than a fixed threshold: $\text{eig}(A - BK) \leq -10$. Although this constraint is independent of the state, it can be evaluated before each experiment and parameters can be rejected if the criterion is not fulfilled. As states, we consider the end-effector position relative to s_{des} and velocity. The parameters we optimize over are q_c, r . The value for κ_d is heuristically set to 0.1 based on our observations of the simulation.

We observe that the underlying functions f, g_i illustrate non-smooth behaviour. Therefore we use the Matérn kernel [35] with parameter $\nu = 3/2$ for our GP. Furthermore, as in practice we cannot run experiments for an infinite horizon, we pick a horizon of $T = 2000$ steps. However, as the problem is not infinite horizon, we only collect the states visited during the initial 500 time steps. Given that the horizon is considerably larger than 500, we consider

these initial states to be safe if the experiment was safe. Additionally, even though we collect the initial 500 states, a lot of them in general would lie close-by. Hence, we sample 50 out of 500 collected data uniformly at random and add them to our GP. Therefore, per experiment, we collect 50 data points.

We restrict our parameter search space to a normalized domain $q_n \times r_n \in [1/3, 1] \times [-1, 1]$ with $q_c = 6q_n$ and $r = 3r_n$.

We initialize SAFEOPT with a policy in the lower half of the safe set (see Fig. 9), i.e., $S_0 = \{(5, -2.7), (4, -3), (6, -2)\}$. Furthermore, we normalize the rewards and the constraint values and therefore pick $\kappa_i = 1$ for the kernel. We proceed similarly for GOSAFEOPT.

B.2. Hardware Results

For the hardware task we apply the following controller:

$$u(x(t)) = -K \begin{bmatrix} s(t) - s_{\text{des}}(t) \\ \dot{x} \end{bmatrix} + \Gamma(q, \dot{q})\dot{s} + \eta(q). \quad (\text{B.4})$$

Furthermore, we define the subsequent reward and constraint functions:

$$\begin{aligned} \mathcal{R}(x(t)) &= -\|s(t) - s_{\text{des}}(t)\|_2, \\ \bar{g}(s(t)) &= \|s(t) - s_w\|_{P,\infty} - \psi, \end{aligned}$$

where s_w represents the center of the wall in Fig. 8 and $\|s - s_w\|_{P,\infty} \leq d_w$ defines the rectangular shaped outline around the wall and $\psi > d_w$.

For the task, we use a squared exponential (SE) kernel [35]. Additionally, due to the symmetric nature of the trajectory, we consider all the states visited during an experiment to be safe. In particular, by choosing the last state of our trajectory to be a terminal state, we can assume the problem has an infinite horizon. Lastly, we sample 100 points at random from the collected rollout and add them to our respective GPs.

C. Additional Definitions

In this section, we present some of the definitions from SAFE_{OPT} and GOSAFE for completeness.

Definition 7. The expanders \mathcal{G}_n are defined as $\mathcal{G}_n := \{a \in S_n \mid e_n(a) > 0\}$ with $e_n(a) = |\{a' \in \mathcal{A} \setminus S_n, \exists i \in \mathcal{I}_g : u_n(a, i) - L_a \|a - a'\| \geq 0\}|$.

Definition 8. The maximizers \mathcal{M}_n are defined as $\mathcal{M}_n := \{a \in S_n \mid u_n(a, 0) \geq \max_{a' \in S_n} l_n(a', 0)\}$.

Definition 9. GOSAFE's discretized state space is defined as $\mathcal{X}_\mu: \forall x \in \mathcal{X}, \exists [x]_\mu \in \mathcal{X}_\mu$ with $\|x - [x]_\mu\|_1 \leq \mu$, where $[x]_\mu$ is the state in \mathcal{X}_μ closest to x in the ℓ_1 -norm.

Definition 10. The safe set S_n in the joint parameter and state space is defined as

$$S_n := S_{n-1} \cup \left(\bigcap_{i \in \mathcal{I}_g} \bigcup_{(a, \tilde{x}_0) \in S_{n-1}} \{(a', \tilde{x}'_0) \in \mathcal{A} \times \mathcal{X}_\mu \mid l_n(a, \tilde{x}_0, i) - L_a \|a - a'\|_1 - L_x (\|\tilde{x}_0 - \tilde{x}'_0\|_1 + \mu) \geq 0\} \right). \quad (\text{C.1})$$

D. Hyperparameters

The hyperparameters of our simulated and real-world experiments are provided in Tables D.2 and D.3.

Table D.2: Hyperparameters of the simulation task

	SAFEOPT	GoSAFEOPT
Iterations	200	200
$\beta_n^{1/2}$	4	4
a lengthscale	0.12,0.12	0.12,0.12
κ for f and g	1, 1	1, 1
σ for f and g	0.1,0.1	0.1,0.1
x lengthscale	-	0.3,0.3,0.3, 2.5,2.5,2.5
ϵ	-	0.1
max LSE steps	-	30
max GE steps	-	10
κ_l	-	0.90
κ_u	-	0.94
η_l	-	0.4
η_u	-	0.6
n_{\max}	-	1000
m	-	500

Table D.3: Hyperparameters of hardware task

	SAFEOPTSWARM	GoSAFEOPT
Iterations	50	50
$\beta_n^{1/2}$	3	3
a lengthscale	0.1,0.1,0.1	0.1,0.1,0.1
κ for f and g	1, 1	1, 1
σ for f and g	0.05,0.3	0.05,0.3
x lengthscale	-	0.3,0.3,0.2, 0.5,0.5,0.3
ϵ	-	0.01
max LSE steps	-	20
max GE steps	-	5
κ_l	-	0.90
κ_u	-	0.94
η_l	-	0.9
η_u	-	1.1
n_{\max}	-	1000
m	-	500